



HAL
open science

Clarifying inflation models: The precise inflationary potential from effective field theory and the WMAP data

D. Cirigliano, Hector J. de Vega, Norma G. Sánchez

► To cite this version:

D. Cirigliano, Hector J. de Vega, Norma G. Sánchez. Clarifying inflation models: The precise inflationary potential from effective field theory and the WMAP data. *Physical Review D*, 2005, 71, pp.103518. 10.1103/PhysRevD.71.103518 . hal-03730848

HAL Id: hal-03730848

<https://hal.science/hal-03730848>

Submitted on 27 Aug 2022

HAL is a multi-disciplinary open access archive for the deposit and dissemination of scientific research documents, whether they are published or not. The documents may come from teaching and research institutions in France or abroad, or from public or private research centers.

L'archive ouverte pluridisciplinaire **HAL**, est destinée au dépôt et à la diffusion de documents scientifiques de niveau recherche, publiés ou non, émanant des établissements d'enseignement et de recherche français ou étrangers, des laboratoires publics ou privés.

Clarifying inflation models: The precise inflationary potential from effective field theory and the WMAP data

D. Cirigliano,¹ H. J. de Vega,^{1,2,*} and N. G. Sanchez^{1,†}¹*Observatoire de Paris, LERMA, Laboratoire Associé au CNRS UMR 8112, 61, Avenue de l'Observatoire, 75014 Paris, France*²*LPTHE, Laboratoire Associé au CNRS UMR 7589, Université Pierre et Marie Curie (Paris VI) et Denis Diderot (Paris VII), Tour 24, 5^{ème}. étage, 4, Place Jussieu, 75252 Paris, Cedex 05, France*

(Received 28 December 2004; published 23 May 2005)

We clarify inflaton models by considering them as effective field theories in the Ginzburg-Landau spirit. In this new approach, the precise form of the inflationary potential is constructed from the present WMAP data, and a useful scheme is prepared to confront with the forthcoming data. In this approach, the WMAP statement excluding the pure ϕ^4 potential implies the presence of an inflaton mass term at the scale $m \sim 10^{13}$ GeV. Chaotic, new and hybrid inflation models are studied in an unified way. In all cases the inflaton potential takes the form $V(\phi) = m^2 M_{\text{Pl}}^2 v(\phi/M_{\text{Pl}})$, where all coefficients in the polynomial $v(\varphi)$ are of order one. If such potential corresponds to supersymmetry breaking, the corresponding susy breaking scale is $\sqrt{m M_{\text{Pl}}} \sim 10^{16}$ GeV which turns to coincide with the grand unification (GUT) scale. The inflaton mass is therefore given by a seesaw formula $m \sim M_{\text{GUT}}^2/M_{\text{Pl}}$. The observables turn to be two-valued functions: one branch corresponds to new inflation and the other to chaotic inflation, the branch point being the pure quadratic potential. For red tilted spectrum, the potential which fits the best the present data ($|1 - n_s| \lesssim 0.1$, $r \lesssim 0.1$) and which best prepares the way for the forthcoming data is a trinomial polynomial with negative quadratic term (new inflation). For blue tilted spectrum, hybrid inflation turns to be the best choice. In both cases we find an analytic formula relating the inflaton mass with the ratio r of tensor to scalar perturbations and the spectral index n_s of scalar perturbations: $10^6(m/M_{\text{Pl}}) = 127\sqrt{r|1 - n_s|}$ where the numerical coefficient is fixed by the WMAP amplitude of adiabatic perturbations. Implications for string theory are discussed.

DOI: 10.1103/PhysRevD.71.103518

PACS numbers: 98.80.Cq, 11.10.-z, 98.70.Vc

I. INTRODUCTION

Inflation was originally proposed to solve several outstanding problems of the standard big bang model [1–5] thus becoming an important paradigm in cosmology. At the same time, inflation provides a natural mechanism for the generation of scalar density fluctuations that seed large scale structure, thus explaining the origin of the temperature anisotropies in the cosmic microwave background (CMB) [6], as well as the tensor perturbations (primordial gravitational waves). Recently, the Wilkinson Microwave Anisotropy Probe (WMAP) collaboration has provided a full-sky map of the temperature fluctuations of the cosmic microwave background (CMB) with unprecedented accuracy and an exhaustive analysis of the data confirming the basic and robust predictions of inflation [7].

During inflation quantum vacuum fluctuations are generated with physical wavelengths that grow faster than the Hubble radius, when the wavelengths of these perturbations cross the horizon they freeze out and decouple [2,4,5]. Wavelengths that are of cosmological relevance today re-enter the horizon during the matter dominated era when the scalar (curvature) perturbations induce temperature anisotropies imprinted on the CMB at the last scattering surface [8,9]. Generic inflationary models predict that

these are mainly Gaussian and adiabatic perturbations with an almost scale invariant spectrum. These generic predictions are in spectacular agreement with the CMB observations as well as with a variety of large scale structure data [7]. The WMAP data [7] clearly display an anticorrelation peak in the temperature-polarization (TE) angular power spectra at $l \sim 150$, providing one of the most striking confirmations of adiabatic fluctuations as predicted by inflation [7].

The classical dynamics of the inflaton (a massive scalar field) coupled to a cosmological background clearly shows that inflationary behavior is an attractor [10]. This is a generic and robust feature of inflation. The robust predictions of inflation (value of the entropy of the universe, solution of the flatness problem, small adiabatic Gaussian density fluctuations explaining the CMB anisotropies, ...) which are common to many available inflationary scenarios, show the predictive power of the inflationary paradigm. Whatever the microscopic model for the early universe (GUT theory) would be, it should include inflation with the generic features we know today.

Inflationary dynamics is typically studied by treating the inflaton as a homogeneous classical scalar field [2–4] whose evolution is determined by a classical equation of motion, while the inflaton quantum fluctuations (around the classical value and in the Gaussian approximation) provide the seeds for the scalar density perturbations of the metric. In quantum field theory, this classical inflaton

*Electronic address: devega@lpthe.jussieu.fr†Electronic address: Norma.Sanchez@obspm.fr

corresponds to the expectation value of a quantum field operator in a translational invariant state. Important aspects of the inflationary dynamics, as resonant particle production and the nonlinear back-reaction that it generates, require a full quantum treatment of the inflaton for their consistent description. The quantum dynamics of the inflaton in a nonperturbative framework and its consequences on the CMB anisotropy spectrum were treated in Refs. [11,12]. Particle decay in de Sitter background and during slow-roll inflation is studied in Ref. [13] together with its implication for the decay of the density fluctuations.

Inflation as known today should be considered as an effective theory, that is, it is not a fundamental theory but a theory of a condensate (the inflaton field) which follows from a more fundamental one (the GUT model). The inflaton field ϕ may not correspond to any real particle (even unstable) but is just an effective description while the microscopic description should come from the GUT model. At present, there is no derivation of the inflaton model from the microscopic GUT theory. However, the relation of inflation to the GUT theory is like the relation of the effective Ginzburg-Landau theory of superconductivity with the microscopic BCS theory. Or like the relation of the $O(4)$ sigma model, an effective particle theory for low energy, with the microscopic quantum chromodynamics (QCD).

The aim of this paper is to provide a clear understanding of inflation and the inflaton potential from effective field theory and the WMAP data. This clearly places inflation within the perspective and understanding of effective theories in particle physics. In addition, it sets up a clean way to directly confront the inflationary predictions with the forthcoming CMB data and select a definitive model.

The following inflaton potential or alternatively the hybrid inflation model are rich enough to describe the physics of inflation and accurately reproduce the available data [7]:

$$V(\phi) = |m^2| M_{\text{Pl}}^2 \left[v_0 \pm \frac{1}{2} \varphi^2 + \frac{2}{3} \gamma \varphi^3 + \frac{1}{32} \kappa \varphi^4 \right]. \quad (1.1)$$

Here $\varphi \equiv \phi/M_{\text{Pl}}$, $|m| \sim 10^{13}$ GeV, the dimensionless parameters γ and κ are of order one, and v_0 is such that $V(\phi)$ and $V'(\phi)$ vanish at the absolute minimum of $V(\phi)$. This ensures that inflation ends after a finite time with a finite number of e-folds. κ must be positive to ensure stability while γ and the mass term φ^2 can have either sign. γ describes how asymmetric is the potential while κ determines how steep it is. Notice that there is no fine-tuning here once the mass scale $|m|$ is fixed.

The potential Eq. (1.1) cover a wide class of inflationary scenarios: small field scenarios (new inflation) for spontaneously broken symmetric potentials (negative mass square), as well as large field scenarios (chaotic inflation) for unbroken symmetric potentials (positive mass square).

Coupling the inflaton to another scalar field yields the hybrid type scenarios.

In the context of an effective theory or Ginzburg-Landau model it is highly unnatural to drop the quadratic term φ^2 . This is to exactly choose the critical point of the model $m^2 = 0$. In fact, the recent WMAP [7] statement unfavoring the monomial φ^4 potential just supports a generic polynomial inflaton potential as in Eq. (1.1). Excluding the quadratic mass term in the potential $V(\phi)$ implies to fine-tune to zero the mass term which is only justified at isolated (critical) points. Therefore, from a physical point of view, the pure quartic potential φ^4 is a weird choice implying to fine-tune to zero the coefficient of φ^2 .

We obtain analytic and unifying expressions for chaotic and new inflation for the relevant observables: the amplitude for scalar fluctuations $|\delta_{kad}^{(S)}|^2$, spectral index n_s and ratio r of tensor to scalar perturbations as well as for hybrid inflation and plot them for the three scenarios. Particularly interesting are the plots of n_s vs. r (Figs. 7 and 18–21).

We express the ratio of the inflaton mass and the Planck mass $x \equiv 10^6(m/M_{\text{Pl}})$ in terms of the amplitude of adiabatic perturbations and the parameters in the potential. Furthermore, we can express x in terms of observable quantities as r and n_s . We find for new inflation when both r and $|n_s - 1|$ are small,

$$x = 5\pi\sqrt{3}10^5 |\delta_{kad}^{(S)}| \sqrt{r(1-n_s)} = 127\sqrt{r(1-n_s)} \pm 6\%. \quad (1.2)$$

where the $\pm 6\%$ correspond to the error bars in the amplitude of adiabatic perturbations[7]. From Figs. 9, 12, and 15 we can understand how the mass ratio m/M_{Pl} varies with n_s and r . We find a limiting value $x_0 \equiv 10^6(m_0/M_{\text{Pl}}) \approx 0.1$ for the inflaton mass such that $m_0 \approx 10^{-7}M_{\text{Pl}}$ is a minimal inflaton mass in order to keep n_s and r within the WMAP data.

New inflation arises for broken symmetric potentials (the minus sign in front of the φ^2 term) while chaotic inflation appears both for unbroken and broken symmetric potentials. For broken symmetry, we find that analytic continuation connects the observables for chaotic and new inflation: the observables are two-valued functions of $y \equiv \kappa N$. (N being the number of e-folds from the first horizon crossing to the end of inflation). One branch corresponds to new inflation and the other branch to chaotic inflation. As shown in Figs. 4–7, 9, 12, and 15, n_s , r and $|\delta_{kad}^{(S)}|^2$ for chaotic inflation are connected by analytic continuation to the same quantities for new inflation. The branch point where the two scenarios connect corresponds to the monomial $+\frac{1}{2}\varphi^2$ potential ($\kappa = \gamma = 0$).

The potential which best fits the present data for a red tilted spectrum ($n_s < 1$) and which best prepares the way to the expected data (a small $r \lesssim 0.1$) is given by the trinomial potential Eq. (1.1) with a negative φ^2 term, that is new inflation.

In new inflation we have the upper bound

$$r \leq \frac{8}{N} \approx 0.16.$$

This upper bound is attained by the quadratic monomial. On the contrary, in chaotic inflation for both signs of the φ^2 term, r is bounded as

$$0.16 \approx \frac{8}{N} < r < \frac{16}{N} \approx 0.32,$$

This bound holds for all values of the cubic coupling γ which describes the asymmetry of the potential. The lower and upper bounds for r are saturated by the quadratic and quartic monomials, respectively.

For chaotic and new inflation, we find the following properties:

(i) n_s is bounded as

$$n_s \leq 1 - \frac{2}{N} \approx 0.96 \quad \text{chaotic inflation,}$$

$$n_s \leq 1 - \frac{1.558005 \dots}{N} \approx 0.9688 \quad \text{new inflation.}$$

The value at the bound for chaotic inflation corresponds to the quadratic monomial.

(ii) n_s decreases with the steepness κ for fixed asymmetry $h \equiv \gamma\sqrt{8/\kappa} < 0$ and grows with the asymmetry $|h|$ for fixed steepness κ .

For chaotic inflation r grows with the steepness κ for fixed asymmetry $h < 0$ and decreases with the asymmetry $|h|$ for fixed steepness κ . Also, in chaotic inflation r decreases with n_s .

For new inflation r does the opposite: it decreases with the steepness κ for fixed asymmetry $h < 0$ while it grows with the asymmetry $|h|$ for fixed steepness κ . Also, in new inflation r grows with n_s .

All this is valid for the general trinomial potential Eq. (1.1) and can be seen in Figs. 7, 18, 20, and 21. In addition, r decreases for increasing asymmetry $|h|$ at a fixed n_s in new inflation (with $h < 0$). As a consequence, the trinomial potential Eq. (1.1) can yield very small r for red tilt with $n_s < 1$ and near unit for new inflation.

Hybrid inflation always gives a blue tilted spectrum $n_s > 1$ in the Λ -dominated regime, allowing $n_s - 1$ and r to be small. Interestingly enough, we obtain for hybrid inflation a formula for the mass ratio x with a similar structure to Eq. (1.2) for new inflation:

$$x = 10^6 \frac{m}{M_{\text{Pl}}} = 127 \sqrt{r \left(n_s - 1 + \frac{3}{8} r \right)}.$$

This is plotted in Figs. 22 and 23 showing that m/M_{Pl} decreases when r and $n_s - 1$ both approach zero. We relate the cosmological constant in the hybrid inflation Lagrangian with the ratio r as

$$\frac{\Lambda_0}{M_{\text{Pl}}^4} = 0.329 \times 10^{-7} r,$$

and we find that $(n_s - 1)$ gives an upper bound on the cosmological constant:

$$\frac{\Lambda_0}{m^2 M_{\text{Pl}}^2} < \frac{2}{n_s - 1}.$$

In order to reproduce the CMB data, the inflationary potentials in the slow-roll scenarios considered in this article must have the structure

$$V(\phi) = M^4 v \left(\frac{\phi}{M_{\text{Pl}}} \right),$$

where $v(0) = v'(0) = 0$ and all higher derivatives at the origin are of the order one. The inflaton mass is therefore given by a seesaw-like formula

$$m \approx \frac{M^2}{M_{\text{Pl}}}. \quad (1.3)$$

As stated above, the WMAP data imply $m \sim 10^{13}$ GeV, Eq. (1.3) implies that M is precisely at the grand unification scale $M \sim 10^{16}$ GeV [2–4]. Three strong independent indications of this scale are available nowadays: 1) the convergence of the running electromagnetic, weak and strong couplings, 2) the large mass scale to explain the neutrino masses via the seesaw mechanism and 3) the scale M in the above inflaton potential. Also, notice that Eq. (1.3) has the structure of the moduli potential coming from supersymmetry breaking. Therefore, the supersymmetry breaking scale would be at the GUT scale too.

In order to generate inflation in string theory, one needs first to generate a mass scale like m and M_{GUT} related by Eq. (1.3). Without such mass scales there is no hope to generate a realistic cosmology reproducing the observed CMB fluctuations. However, an effective description of inflation in string theory could be at reach [14]

In summary, for small $r \leq 0.1$ and n_s near unit, new inflation from the trinomial potential Eq. (1.1) and hybrid inflation emerge as the best candidates. Whether n_s turns to be above or below unit will choose hybrid or new inflation, respectively. In any case $|n_s - 1|$ turns to be of order $1/N$ (N being the number of e-folds from the first horizon crossing to the end of inflation). This can be understood intuitively as follows: the geometry of the universe is scale invariant during de Sitter stage since the metric takes in conformal time the form

$$ds^2 = \frac{1}{(H\eta)^2} [(d\eta)^2 - (d\vec{x})^2].$$

Therefore, the primordial power generated is scale invariant except for the fact that inflation is not eternal and lasts for N e-folds. Hence, the primordial spectrum is scale invariant up to $1/N$ corrections. Also, the ratio r turns to

be of order $1/N$ (chaotic and new inflation) or $1/N^2$ (hybrid inflation).

II. INFLATION AND THE INFLATON FIELD: AN EFFECTIVE FIELD THEORY

Inflation is part of the standard cosmology since several years. Inflation emerged in the 80s as the only way to explain the ‘‘bigness’’ of the universe, that is, the value of the entropy of the universe today $\sim 10^{90} \sim (e^{69})^3$. Closely related to this, inflation solves the horizon and flatness problem, thus explaining the quasi-isotropy of the CMB. For a recent outlook see [15].

The inflationary era corresponds to the scale of energies of grand unification. It is not yet known which field model appropriately describes the matter at such scales. Fortunately, one does not need a detailed description in order to investigate inflationary cosmology, one needs the expectation value of the quantum energy density (T_{00}) which enters in the r.h.s. of the Einstein-Friedman equation

$$\left[\frac{1}{a(t)} \frac{da}{dt} \right]^2 = \frac{1}{3M_{\text{Pl}}^2} \rho(t), \quad (2.1)$$

This is dominated by field condensates. Since fermion fields have zero expectation values, only the bosonic fields are relevant. Bosonic fields do not need to be fundamental fields, they can describe fermion-antifermion pairs $\langle \bar{\Psi}\Psi \rangle$ in a grand unified theory (GUT). In order to describe the cosmological evolution is enough to consider the effective dynamics of such condensates. In fact, one condensate field is enough to obtain inflation. This condensate field is usually called ‘‘inflaton’’ and its dynamics can be described by a Ginzburg-Landau Lagrangian in the cosmological background

$$ds^2 = dt^2 - a^2(t) d\vec{x}^2 \quad (2.2)$$

That is, an effective local Lagrangian containing terms of dimension less or equal than four in order to be renormalizable,

$$\mathcal{L} = a^3(t) \left[\frac{\dot{\phi}^2}{2} - \frac{(\nabla\phi)^2}{2a^2(t)} - V(\phi) \right]. \quad (2.3)$$

Here, the inflaton potential $V(\phi)$ is often taken as a quartic polynomial: $V(\phi) = (m^2/2)\phi^2 + (\lambda/4)\phi^4$.

The Einstein-Friedman Eq. (2.1) for homogeneous fields take the form

$$H^2(t) = \frac{1}{3M_{\text{Pl}}^2} \left[\frac{\dot{\phi}^2}{2} + V(\phi) \right], \quad H(t) \equiv \frac{1}{a(t)} \frac{da}{dt} \quad (2.4)$$

where we used Eq. (2.3), and $H(t)$ stands for the Hubble parameter.

The inflaton field ϕ may not correspond to any real particle (even unstable) but is just an effective description of the dynamics. The detailed microscopical description should be given by the GUT. Somehow, the inflaton is to

the microscopic GUT theory what the Ginzburg-Landau effective theory of superconductivity is to the microscopic BCS theory. Another relevant example of effective field theory in particle physics is the $O(4)$ sigma model which describes quantum chromodynamics (QCD) at low energies [16]. The inflaton model can be thus considered as an effective theory. That is, it is not a fundamental theory but a theory on the condensate (the inflaton field) which follows from a more fundamental theory (the GUT model), by integrating over the basic fields in the latter. In principle, it should be possible to derive the inflaton Lagrangian from a GUT model including GUT fermions and gauge fields. Although, such derivation is not yet available, one can write down, as in the case of the sigma model describing the low energy behavior of QCD, the effective Lagrangian for the particles of interest (the pions, the sigma and photons) without explicit calculation in the fundamental theory. The guiding principle being the symmetries to be respected by the effective model [16]. Contrary to the sigma model where the chiral symmetry strongly constrains the model[16], only Lorentz invariance can be imposed to the inflaton model. Besides that, one can always eliminate linear terms in the Lagrangian by a constant shift of the inflaton field.

Restricting ourselves to renormalizable theories we can choose a general quartic Lagrangian with

$$V(\phi) = V_0 + \frac{m^2}{2} \phi^2 + \frac{|m|g}{3} \phi^3 + \frac{\lambda}{4} \phi^4. \quad (2.5)$$

where λ and g are dimensionless parameters and V_0 is chosen such that $V(\phi)$ vanishes at its absolute minimum. This ensures that inflation ends after a finite time with a finite number of e-folds. We choose $\lambda > 0$ as a stability condition in order to have a potential bounded from below while m^2 and g may have any sign. An inflaton potential of this type was considered in Ref. [17].

As it is known, in order to reproduce the CMB anisotropies, one has to choose m around the GUT scale $m \sim 10^{-6} M_{\text{Pl}} \sim 10^{13}$ GeV, and the coupling λ very small ($\lambda \sim 10^{-12}$) [2–4] while g may be just omitted.

Let us see that the choice $\lambda \sim 10^{-12}$ is not independent from the value of $m/M_{\text{Pl}} \sim 10^{-6}$. Let us define a dimensionless field $\varphi \equiv \phi/M_{\text{Pl}}$, the potential V for $m^2 > 0$ takes now the form,

$$V(\phi) = m^2 M_{\text{Pl}}^2 \left[\frac{1}{2} \varphi^2 + \frac{1}{3} g \frac{M_{\text{Pl}}}{m} \varphi^3 + \frac{1}{4} \lambda \frac{M_{\text{Pl}}^2}{m^2} \varphi^4 \right] + V_0, \\ \varphi = \frac{\phi}{M_{\text{Pl}}}$$

or

$$V(\varphi) = m^2 M_{\text{Pl}}^2 \left[v_0 + \frac{1}{2} \varphi^2 + \frac{2}{3} \gamma \varphi^3 + \frac{1}{32} \kappa \varphi^4 \right]. \quad (2.6)$$

Here,

$$\gamma \equiv g \frac{M_{\text{Pl}}}{2m}, \quad \kappa \equiv 8\lambda \frac{M_{\text{Pl}}^2}{m^2}, \quad v_0 \equiv \frac{V_0}{m^2 M_{\text{Pl}}^2}, \quad (2.7)$$

are all three of order one in order to reproduce the CMB anisotropies. Hence, once the mass m is chosen to be in the scale $\sim 10^{13}$ GeV, the remaining parameters γ, κ, \dots turn out to be of order one. In other words, there is no fine tuning in the choice of the inflaton self-couplings. γ describes how asymmetric is the potential while κ determines how steep it is.

In typical inflationary scenarios one initially has $V \sim H^2 M_{\text{Pl}}^2$ and $H \sim 5m$. This makes the parametrization $V(\varphi)$ as in Eq. (2.6) very natural with φ less than (or of the order) one at the beginning of inflation.

In the context of an effective theory or Ginzburg-Landau model it is highly unnatural to set $m = 0$. This corresponds to be exactly at the critical point of the model where the mass vanishes, that is, the correlation length is infinite in the statistical mechanical context. In fact, the recent WMAP [7] statement unfavoring the $m = 0$ choice (purely ϕ^4 potential) just supports a generic polynomial inflaton potential possessing a ϕ^2 mass term plus ϕ^4 (plus eventually other terms).

We want to stress that excluding the quadratic mass term in the potential $V(\phi)$ implies to fine-tune to zero the mass term which is only justified at isolated points (a critical point in statistical mechanics). Therefore, from a physical point of view, the pure quartic potential is a weird choice implying to fine-tune to zero the coefficient of the mass term. In other words, one would be considering a field with self-interaction but lacking of the mass term.

Choosing $g = 0$ implies that $\varphi \rightarrow -\varphi$ is a symmetry of the inflaton potential. We do not see reasons based on fundamental physics to choose a zero or a nonzero g . Only the phenomenology, that is the fit to CMB data, can decide for the moment on the value of g .

A model with only one field is clearly unrealistic since the inflaton would then describe a stable and ultraheavy (GUT scale) particle. It is necessary to couple the inflaton with lighter particles, then, the inflaton can decay into them. There are many available scenarios for inflation. Most of them add other fields coupled to the inflaton. This variety of inflationary scenarios may seem confusing since several of them are compatible with the observational data [7]. Indeed, future observations should constraint the models more tightly excluding some families of them. Anyway, the variety of acceptable inflationary models shows the power of the inflationary paradigm. Whatever the correct microscopic model for the early universe would be, it should include inflation with the generic features we know today. In addition, many inflatons can be considered (multifield inflation). Such family of models introduce extra features as nonadiabatic (isocurvature) density fluctuations, which in turn become strongly constrained by the WMAP data [7].

The scenarios where the inflaton is treated classically are usually characterized into small and large fields scenarios. In small fields scenarios the initial classical amplitude of the inflaton is assumed small compared with M_{Pl} , while in large field scenarios the inflaton is initially of the order $\sim M_{\text{Pl}}$ [4]. The first type of scenarios is usually realized with spontaneously broken symmetric potentials ($m^2 < 0$, 'new inflation', also called "small field inflation"), while for the second type scenarios one can just use unbroken potentials ($m^2 > 0$, "chaotic inflation" also called "large field inflation").

We will restrict in this paper to inflationary potentials of degree four as in Eq. (2.6). This ensures that the corresponding quantum theory is renormalizable. Notice that being the inflaton model an effective theory nothing forbids to consider inflationary potentials of arbitrary high order. In general, the potential $V(\phi)$ will have the form:

$$V(\phi) = m^2 M_{\text{Pl}}^2 v\left(\frac{\phi}{M_{\text{Pl}}}\right), \quad (2.8)$$

where $v(0) = v'(0) = 0$ and all higher derivatives at the origin are of the order one. The arbitrary function $v(\varphi)$ allows detailed fits. However, already a quartic potential is rich enough to describe the full physics and to reproduce accurately the data. In such case we have from Eqs. (2.6) and (2.8) for $m^2 > 0$,

$$v(\varphi) = v_0 + \frac{1}{2}\varphi^2 + \frac{2}{3}\gamma\varphi^3 + \frac{1}{32}\kappa\varphi^4.$$

In dimensionless variables the Einstein-Friedman Eq. (2.4) takes the form,

$$h^2(\tau) = \frac{1}{3} \left[\frac{\dot{\varphi}^2}{2} + v(\varphi) \right], \quad (2.9)$$

where we introduced the dimensionless time variable $\tau \equiv mt$, $\dot{\varphi} \equiv d\varphi/d\tau$ and $h(\tau) \equiv H(t)/m$.

The evolution equation for the field $\varphi(\tau)$ then reads

$$\ddot{\varphi} + 3h\dot{\varphi} + v'(\varphi) = 0. \quad (2.10)$$

In the case of the quartic potential Eqs. (2.9) and (2.10) become,

$$h^2(\tau) = \frac{1}{6} \left[\dot{\varphi}^2 + \varphi^2 + \frac{2}{3}\gamma\varphi^3 + \frac{1}{16}\kappa\varphi^4 + 2v_0 \right], \quad (2.11)$$

$$\ddot{\varphi} + 3h\dot{\varphi} + \varphi + 2\gamma\varphi^2 + \kappa\varphi^3 = 0.$$

We similarly treat the spontaneous symmetry breaking case $m^2 < 0$ by setting

$$V(\phi) = |m|^2 M_{\text{Pl}}^2 v(\varphi) \quad \text{where} \quad (2.12)$$

$$v(\varphi) = -\frac{1}{2}\varphi^2 + \frac{2}{3}\gamma\varphi^3 + \frac{1}{32}\kappa\varphi^4 + v_0.$$

and

$$\gamma \equiv g \frac{M_{\text{Pl}}}{2|m|}, \quad \kappa \equiv 8\lambda \frac{M_{\text{Pl}}^2}{|m^2|}, \quad v_0 \equiv \frac{V_0}{|m^2|M_{\text{Pl}}^2}, \quad (2.13)$$

instead of Eqs. (2.6) and (2.7). In the case $m^2 < 0$ the minimum of the potential is not at the origin but the second derivative of $v(\varphi)$ at its absolute minimum is always positive. That is, the physical mass square of the inflaton field is positive whatever the sign of m^2 .

We restrict ourselves to potentials $V(\phi)$ which are polynomials of degree four in ϕ . Higher order polynomials describe nonrenormalizable interactions, although being acceptable as effective field theories [16]. As we show below, already quartic polynomials for $V(\phi)$ are rich enough to describe the full physics and fit the present data. One could use higher order polynomials to refine the fits.

III. DENSITY FLUCTUATIONS: CHAOTIC INFLATION AND NEW INFLATION

We present here the density fluctuations for a general inflationary potential as in Eq. (2.6). Scalar and tensor perturbations in inflation have been the subject of intense activity [4,5,8,9] in particular, their contrast with the WMAP data [7,18]

A. The binomial inflaton potential

Let us start with the case where the potential is just a binomial in φ^2 . We have for the unbroken symmetry case $m^2 > 0$,

$$v_{ub}(\varphi) = \frac{1}{2}\varphi^2 + \frac{1}{32}\kappa\varphi^4. \quad (3.1)$$

and for the symmetry breaking case $m^2 < 0$,

$$v_b(\varphi) = \frac{\kappa}{32}\left(\varphi^2 - \frac{8}{\kappa}\right)^2 = -\frac{1}{2}\varphi^2 + \frac{1}{32}\kappa\varphi^4 + \frac{2}{\kappa}. \quad (3.2)$$

where κ is defined by Eq. (2.13). The value of v_0 is chosen such that $v = 0$ at its absolute minimum ($v_0 = 0$ for v_{ub} and $v_0 = 2/\kappa$ for v_b). This ensures that inflation ends after a finite time with a finite number of e-folds.

The chaotic scenario is realized for $m^2 > 0$ with the inflaton starting at some value φ of the order one, ($0 < \varphi < +\infty$). By the end of inflation φ is near the minimum of the potential at $\varphi = \varphi_0 = 0$ (see Fig. 1).

The new inflationary scenario is realized for $m^2 < 0$ with the symmetry breaking potential Eq. (3.2) and the initial condition φ very close to the origin $\varphi = 0$, ($0 < \varphi < \varphi_0 = \sqrt{8/\kappa}$), where φ_0 is the minimum of the potential. By the end of inflation, φ is near φ_0 (see Fig. 1).

In addition, one obtains chaotic inflation in the case $m^2 < 0$ choosing the initial φ larger than φ_0 , ($\varphi_0 < \varphi < +\infty$).

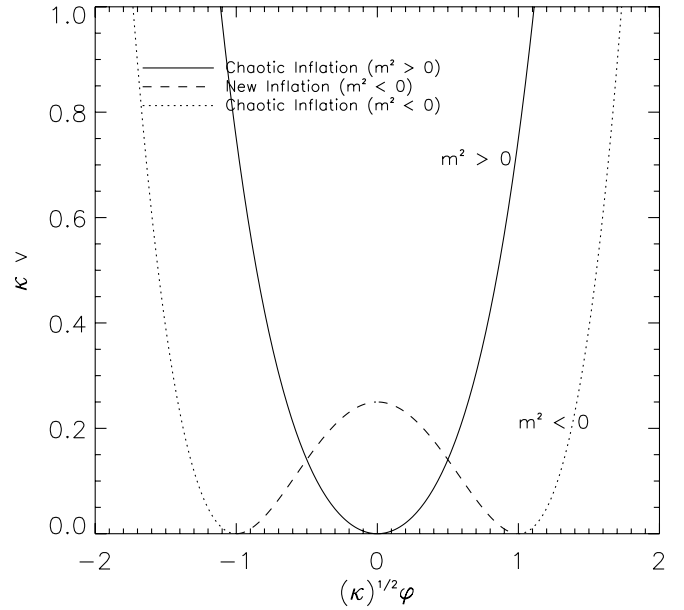


FIG. 1. The binomial potential Eqs. (3.1) and (3.2) for both unbroken and broken cases: $\kappa v_{ub}(\varphi)(m^2 > 0)$ and $\kappa v_b(\varphi)(m^2 < 0)$ vs. $\sqrt{\frac{\kappa}{8}}\varphi$.

We display in Fig. 1 the binomial potentials $\kappa v_{ub}(\varphi)$ and $\kappa v_b(\varphi)$ as functions of $\sqrt{\frac{\kappa}{8}}\varphi$.

In the slow-roll approximation valid for $\dot{\varphi} \ll \varphi$ we can approximate the number of e-folds from the time τ until the end of inflation as

$$\begin{aligned} N(\tau) &= \int_{\tau}^{\tau_0} h(\tau) d\tau = -3 \int_{\varphi(\tau)}^{\varphi_0} \frac{h^2}{v'(\varphi)} d\varphi \\ &= - \int_{\varphi(\tau)}^{\varphi_0} \frac{v(\varphi)}{v'(\varphi)} d\varphi. \end{aligned} \quad (3.3)$$

where φ_0 is the inflaton field by the end of inflation. That is, modes with comoving wavenumber $k = mh(\tau)a(\tau)$ cross the horizon for the first time at the time τ , $N(\tau)$ e-folds before the end of inflation.

The spectral indices and r can be expressed in terms of the slow-roll parameters as [9],

$$n_s = 1 - 6\epsilon + 2\eta, \quad r = 16\epsilon \quad (3.4)$$

where to dominant order in slow roll,

$$\begin{aligned} \epsilon &= \frac{1}{2} M_{\text{Pl}}^2 \left(\frac{V'}{V} \right)^2 = \frac{1}{2} \left(\frac{v'(\varphi)}{v(\varphi)} \right)^2, \\ \eta &= M_{\text{Pl}}^2 \frac{V''}{V} = \frac{v''(\varphi)}{v(\varphi)}. \end{aligned} \quad (3.5)$$

The amplitude of adiabatic perturbations is expressed as

$$|\delta_{kad}^{(S)}|^2 = \frac{1}{12\pi^2 M_{\text{Pl}}^6} \frac{V^3}{V'^2} = \frac{1}{12\pi^2} \frac{|m^2|}{M_{\text{Pl}}^2} \frac{v^3(\varphi)}{v'^2(\varphi)}. \quad (3.6)$$

As explained above, we can take $\varphi_0 = 0$ for chaotic inflation while for new inflation $\varphi_0 = 1/\sqrt{\kappa}$. We obtain in this way inserting Eqs. (3.1) and (3.2) into Eq. (3.3),

$$\kappa N(\varphi) = \frac{\kappa}{8} \varphi^2 + \log \left[1 + \frac{\kappa}{8} \varphi^2 \right] \quad m^2 > 0 \quad (3.7)$$

and

$$\kappa N(\varphi) = \frac{\kappa}{8} \varphi^2 - 1 - \log \left[\frac{\kappa}{8} \varphi^2 \right] \quad m^2 < 0. \quad (3.8)$$

Equations (3.7) and (3.8) can be written in an unified form by introducing the new variables z_{ub} and z_b

$$z_{ub} \equiv 1 + \frac{\kappa}{8} \varphi^2, \quad z_b \equiv \frac{\kappa}{8} \varphi^2, \quad \kappa = 8\lambda \frac{M_{\text{Pl}}^2}{|m^2|}. \quad (3.9)$$

That is,

$$\begin{aligned} \kappa N(\varphi) &= z_{ub} - 1 + \log z_{ub} \quad m^2 > 0, \\ \kappa N(\varphi) &= z_b - 1 - \log z_b \quad m^2 < 0, \end{aligned} \quad (3.10)$$

and we have

$$1 < z_{ub} < \infty, \quad \text{chaotic inflation} \quad m^2 > 0,$$

$$0 < z_b < 1, \quad \text{new inflation} \quad m^2 < 0,$$

$$1 < z_b < \infty, \quad \text{chaotic inflation} \quad m^2 < 0.$$

Using Eqs. (3.5) n_s and r can be expressed in terms of z_{ub} and z_b

$$\begin{aligned} m^2 > 0 : \quad n_s &= 1 - \kappa \frac{3z_{ub}^2 - z_{ub} + 2}{(z_{ub} - 1)(z_{ub} + 1)^2}, \\ r &= 16\kappa \frac{z_{ub}^2}{(z_{ub} - 1)(z_{ub} + 1)^2}; \end{aligned} \quad (3.11)$$

$$\begin{aligned} m^2 < 0 : \quad n_s &= 1 - \kappa \frac{3z_b + 1}{(z_b - 1)^2}, \\ r &= 16\kappa \frac{z_b}{(z_b - 1)^2}, \end{aligned} \quad (3.12)$$

and the amplitudes of adiabatic perturbations Eq. (3.6) read

$$|\delta_{kad}^{(S)}|^2 = \frac{1}{12\pi^2} \frac{m^2}{M_{\text{Pl}}^2} \frac{(z_{ub} - 1)^2 (z_{ub} + 1)^3}{\kappa^2 z_{ub}^2} \quad m^2 > 0, \quad (3.13)$$

$$|\delta_{kad}^{(S)}|^2 = \frac{1}{12\pi^2} \frac{|m^2|}{M_{\text{Pl}}^2} \frac{(z_b - 1)^4}{\kappa^2 z_b} \quad m^2 < 0. \quad (3.14)$$

The variables z_{ub} and z_b are functions of κ times the number of e-folds N defined by Eqs. (3.7) and (3.8). Hence, Eqs. (3.10), (3.11), and (3.12) provide the spectral indices as functions of κN in a parametric way.

Equations (3.13) and (3.14) permit to express the mass ratio $|m^2|/M_{\text{Pl}}^2$ in terms of the amplitude of adiabatic perturbations, and hence determine $|m^2|/M_{\text{Pl}}^2$ using the WMAP values Δ_{\pm} [7] for $|\delta_{kad}^{(S)}|^2$,

$$\Delta_- \equiv 0.194 < 10^8 |\delta_{kad}^{(S)}|^2 < \Delta_+ \equiv 0.244. \quad (3.15)$$

In terms of the variable,

$$x \equiv 10^6 \frac{m}{M_{\text{Pl}}}, \quad (3.16)$$

the observational bounds Eq. (3.15) imply

$$\frac{200\sqrt{3}\pi}{N} g(z)\sqrt{\Delta_-} < x < \frac{200\sqrt{3}\pi}{N} g(z)\sqrt{\Delta_+}, \quad (3.17)$$

where

$$\begin{aligned} m^2 > 0 : \quad g_{ub}(z_{ub}) &= \frac{\kappa N z_{ub}}{(z_{ub} - 1)(z_{ub} + 1)^{3/2}}; \\ m^2 < 0 : \quad g_b(z_b) &= \frac{\kappa \sqrt{z_b} N}{(z_b - 1)^2}. \end{aligned} \quad (3.18)$$

Recall that κN is a function of z_{ub} or z_b , respectively, according to Eq. (3.10). Notice that the upper and lower bounds $\sqrt{\Delta_{\pm}}$ are quite close[7]:

$$10^4 |\delta_{kad}^{(S)}| = \sqrt{\Delta_{\pm}} = 0.467 \pm 0.027, \quad (3.19)$$

which corresponds to $\pm 6\%$.

For $m^2 > 0$ (chaotic inflation) we plot in Fig. 2 the upper and lower bounds for $x = 10^6(m/M_{\text{Pl}})$ given in Eqs. (3.17)

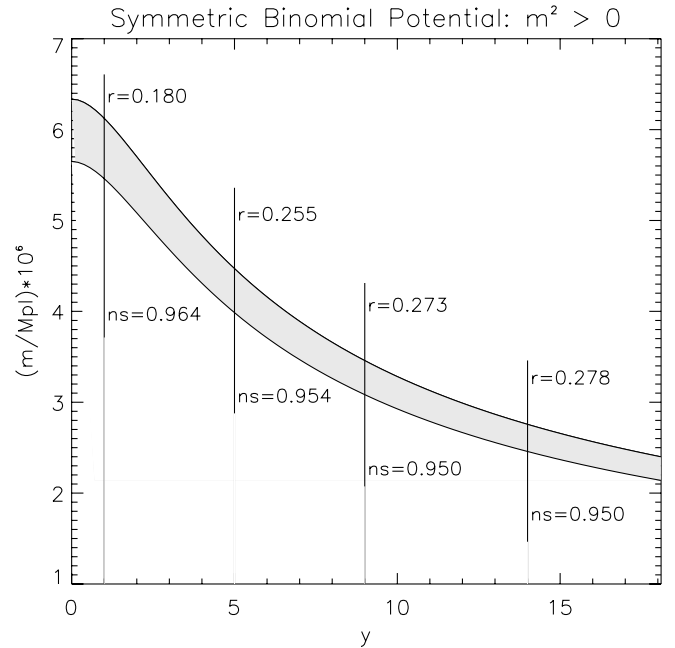


FIG. 2. Upper and lower bounds for the mass ratio $10^6 m/M_{\text{Pl}}$ as functions of $y = \kappa N$ for $m^2 > 0$ (chaotic inflation) for $N = 60$ with the binomial potential Eq. (3.1).

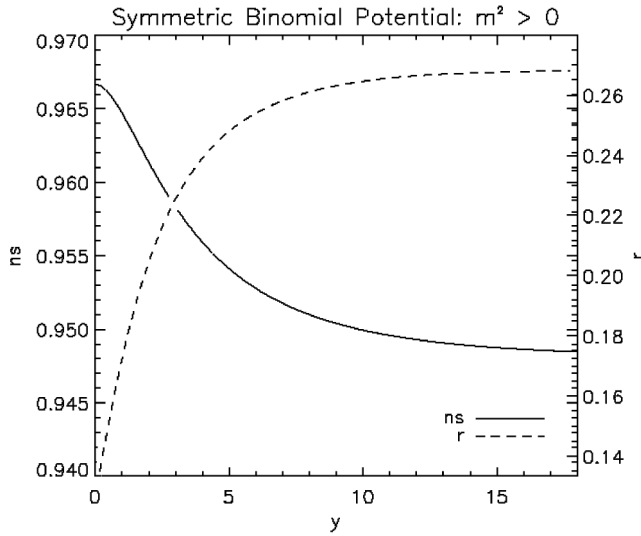


FIG. 3. The scalar index n_s and the ratio r as functions of $y = \kappa N$ for $m^2 > 0$ and $N = 60$ (chaotic inflation), with the binomial potential Eq. (3.1). Both n_s and r monotonically interpolate between their limiting values corresponding to the pure monomials φ^2 and φ^4 .

as functions of κN , and in Fig. 3 we plot n_s and r as functions of κN . We see that both n_s and r for $0 < \kappa N < \infty$ monotonically interpolate between their limiting values given by Eqs. (3.20) and (3.21) corresponding to the purely quadratic and quartic potentials, respectively. We used $N = 60$ in the plots. Very similar results are obtained for $N = 50$.

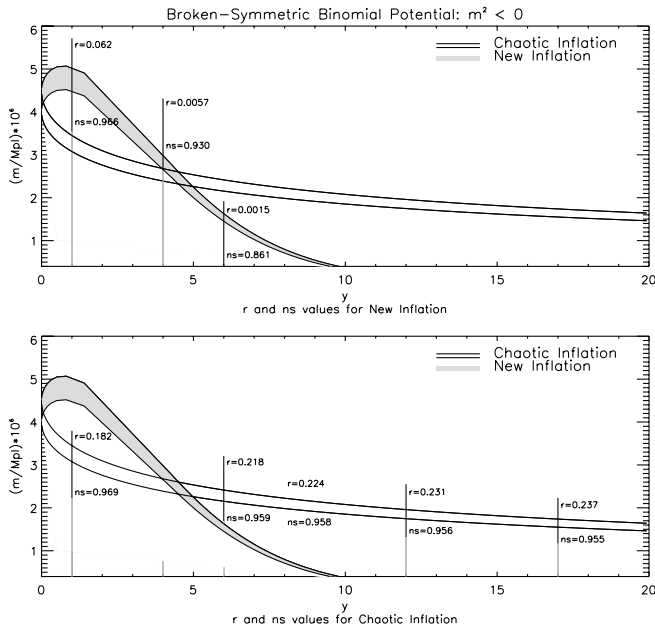


FIG. 4. Upper and lower bounds for $10^6(m/M_{\text{Pl}})$ for $N = 60$ as a function of $y = \kappa N$ with the binomial potential Eq. (3.2) for $m^2 < 0$. Lower branches describe chaotic inflation and upper branches correspond to new inflation.

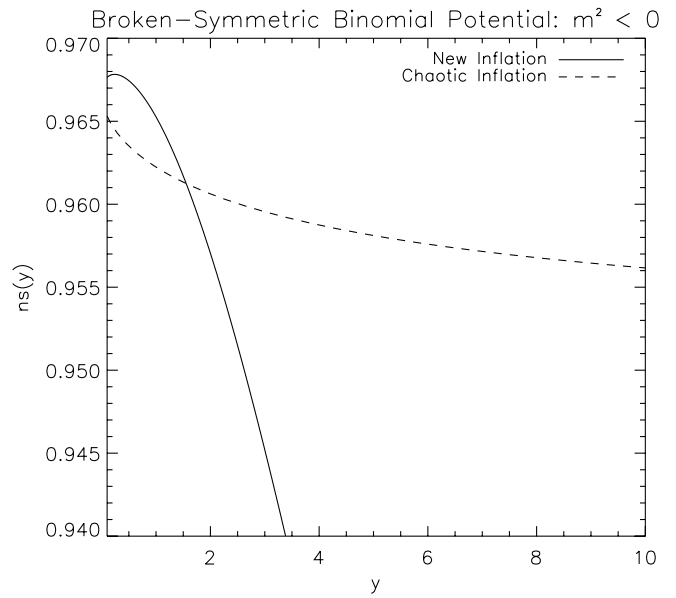


FIG. 5. n_s as a function of $y = \kappa N$ for $m^2 < 0$ and $N = 60$, chaotic and new inflation, with the binomial potential Eq. (3.2).

In Fig. 4 we plot the upper and lower bounds for $x = 10^6(m/M_{\text{Pl}})$ given in Eqs. (3.17) as functions of κN for $m^2 < 0$. Both inflationary scenarios are displayed: new inflation for $0 < z_b < 1$ and chaotic inflation for $1 < z_b < \infty$.

In Figs. 5 and 6 we plot n_s and r as functions of κN for $m^2 < 0$, respectively. We see that n_s and r are two-valued functions of κN . One branch corresponds to new inflation and the other branch to chaotic inflation. $\kappa N = 0$ is a branch point where we recover the results for the purely (monomial) quadratic potential Eq. (3.20). The result for

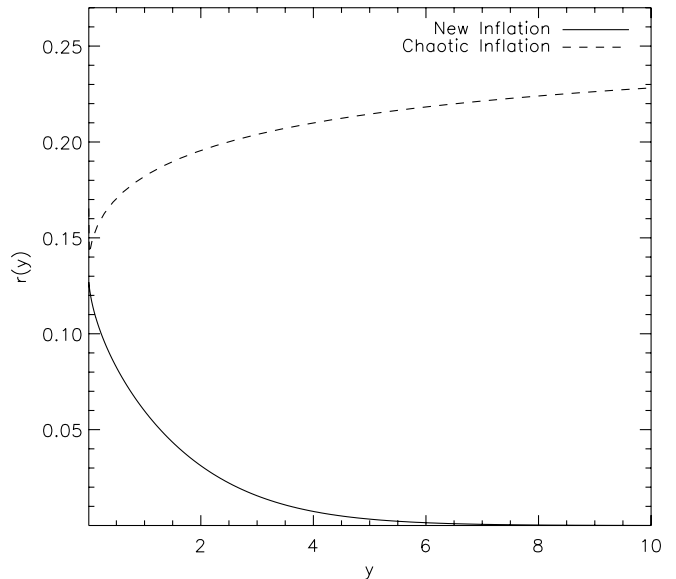


FIG. 6. r as a function of $y = \kappa N$ for $m^2 < 0$ and $N = 60$, chaotic and new inflation, with the binomial potential Eq. (3.2).

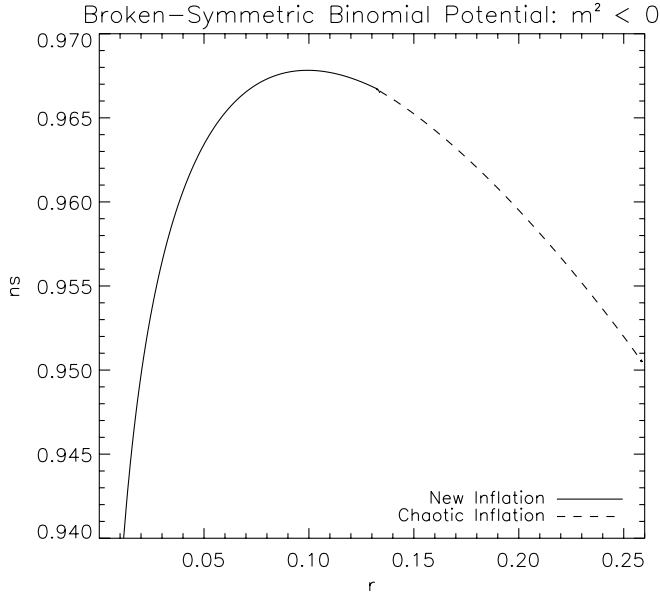


FIG. 7. n_s vs. r for $m^2 < 0$, new and chaotic inflation, with the binomial potential Eq. (3.2).

the purely quartic potential Eq. (3.21) is obtained from the chaotic inflation branch of n_s and r in the $\kappa N \rightarrow \infty$ limit.

We depict in Fig. 7 n_s vs. r for $m^2 < 0$ both for new and chaotic inflation.

$$z_{ub} \stackrel{\kappa \rightarrow +\infty}{=} +\infty, \quad n_s \stackrel{\kappa \rightarrow +\infty}{=} 1 - \frac{3}{N} \approx 0.94,$$

$$r \stackrel{\kappa \rightarrow +\infty}{=} \frac{16}{N} \approx 0.32, \quad \text{chaotic inflation, purely quartic } V(\phi) \quad |\delta_{kad}^{(S)}|^2 \stackrel{\kappa \rightarrow +\infty}{=} \frac{2}{3\pi^2} \frac{N^3 m^2}{M_{\text{Pl}}^2}, \quad g_{ub}(z) \stackrel{\kappa \gg 1}{=} \frac{1}{\sqrt{\kappa N}}. \quad (3.21)$$

For $m^2 < 0$ (i. e. broken symmetry) and $\kappa \rightarrow 0$ we find from Eq. (3.8) that $z_b \rightarrow 1$ and then n_s , r and $|\delta_{kad}^{(S)}|^2$ in Eqs. (3.12) and (3.14) tend to the same values than for the unbroken symmetry case Eq. (3.20).

The limiting case $\kappa \rightarrow \infty$ for broken symmetry and chaotic inflation leads from Eq. (3.10) to $z_b \rightarrow +\infty$ and we recover the same values as in Eq. (3.21) after using Eqs. (3.12) and (3.14).

When $\kappa \rightarrow \infty$ for broken symmetry and new inflation we have from Eq. (3.10),

$$z_b \stackrel{\kappa \gg 1}{=} e^{-\kappa N - 1}.$$

This leads using Eqs. (3.12) and (3.14) to

$$\begin{aligned} n_s \stackrel{\kappa \gg 1}{=} 1 - \kappa, \quad r \stackrel{\kappa \gg 1}{=} 16\kappa e^{-\kappa N - 1}, \quad \text{new inflation,} \quad V(\phi) \stackrel{\kappa \gg 1}{=} \frac{\lambda}{4} \phi^4 \text{ in the limit,} \\ |\delta_{kad}^{(S)}|^2 \stackrel{\kappa \gg 1}{=} \frac{1}{768\pi^2} \frac{m^4}{\lambda M_{\text{Pl}}^4} e^{\kappa N + 1}, \quad g_b(z) \stackrel{\kappa \gg 1}{=} \kappa N e^{-1/2\kappa N - 1/2} \rightarrow 0. \end{aligned} \quad (3.22)$$

In this limit, new inflation yields a very small ratio r together with an index n_s well below unit, while the bound on the inflaton mass Eq. (3.17) becomes very small as compared with M_{Pl} since $g_b(z)$ decreases exponentially with κ .

We see from Fig. 3 that for chaotic inflation and both signs of m^2 ,

1. Limiting cases

Let us now consider limiting cases, first for unbroken symmetry ($m^2 > 0$) and then for broken symmetry ($m^2 < 0$).

The limiting case $\kappa \rightarrow 0$ corresponds to a vanishing quartic coupling [see Eq. (2.7)]. That is, the inflaton potential reduces in this case to the quadratic piece $v(\phi) \rightarrow \frac{1}{2}\phi^2$ for $m^2 > 0$.

For chaotic inflation in the $\kappa \rightarrow 0$ limit we obtain from Eqs. (3.9), (3.10), and (3.11),

$$z_{ub} \kappa \rightarrow 0, \quad n_s \stackrel{\kappa \rightarrow 0}{=} 1 - \frac{2}{N} \approx 0.96, \quad r \stackrel{\kappa \rightarrow 0}{=} \frac{8}{N} \approx 0.16,$$

$$\text{chaotic inflation,} \quad v(\phi) = \frac{1}{2}\phi^2,$$

$$|\delta_{kad}^{(S)}|^2 \stackrel{\kappa \rightarrow 0}{=} \frac{1}{6\pi^2} \frac{N^2 m^2}{M_{\text{Pl}}^2}, \quad g_{ub}(1) = \frac{1}{\sqrt{2}}. \quad (3.20)$$

The opposite limit $\kappa \rightarrow \infty$ corresponds to a vanishing mass m^2 [see Eq. (2.7)]. That is, the inflaton potential becomes in this case purely quartic $V(\phi) \rightarrow \frac{\lambda}{4}\phi^4$.

For chaotic inflation in the $\kappa \rightarrow \infty$ limit we obtain from Eqs. (3.9), (3.10), and (3.11)

$$n_s \leq 1 - \frac{2}{N} \approx 0.96 \quad \text{chaotic inflation,}$$

Figure 5 shows that n_s for new inflation has a maximum at $y = \kappa N = 0.2386517\dots$ and then

$$n_s \leq 1 - \frac{1.558005\dots}{N} \approx 0.9688 \quad \text{new inflation.}$$

Figures 3 and 6 show that for chaotic inflation and both signs of m^2 ,

$$0.16 \simeq \frac{8}{N} < r < \frac{16}{N} \simeq 0.32 \quad \text{chaotic inflation,}$$

while for new inflation ($m^2 < 0$),

$$0 < r < \frac{8}{N} \simeq 0.16 \quad \text{new inflation.}$$

Notice that new inflation can give small values for r with a n_s significantly below unit and a low value for $|m|^2/M_{\text{pl}}^2$ while r in chaotic inflation is bounded from below by $\frac{8}{N} \simeq 0.15$. We come back to this point when analyzing the trinomial inflaton potential in sec. III B below.

B. The trinomial inflaton potential

We consider in this section inflation arising from the trinomial inflaton potential with negative squared mass

$$V(\phi) = |m|^2 M_{\text{pl}}^2 v(\varphi) \quad \text{where}$$

$$v(\varphi) = -\frac{1}{2}\varphi^2 + \frac{2}{3}\gamma\varphi^3 + \frac{1}{32}\kappa\varphi^4 + v_0. \quad (3.23)$$

This potential has three extremes: a local maximum at $\varphi = 0$ and two local minima at $\varphi = \varphi_{\pm}$ where

$$\varphi_+ = \frac{8}{\kappa} \left[\sqrt{\gamma^2 + \frac{\kappa}{8}} - \gamma \right], \quad (3.24)$$

$$\varphi_- = -\frac{8}{\kappa} \left[\sqrt{\gamma^2 + \frac{\kappa}{8}} + \gamma \right].$$

The absolute minimum of $v(\varphi)$ is at $\varphi = \varphi_-$ for $\gamma > 0$ and at $\varphi = \varphi_+$ for $\gamma < 0$. We choose v_0 such that $v(\varphi)$ vanishes at its absolute minimum. Such condition gives,

$$v_0 = \frac{2}{\kappa} w(h) \quad \text{where}$$

$$w(h) \equiv \frac{8}{3}h^4 + 4h^2 + 1 + \frac{8}{3}|h|\Delta^3, \quad (3.25)$$

$$h \equiv \gamma \sqrt{\frac{8}{\kappa}} \quad \text{and} \quad \Delta \equiv \sqrt{h^2 + 1}.$$

The parameter h reflects how asymmetric is the potential. Notice that $v(\varphi)$ is invariant under the changes $\varphi \rightarrow -\varphi$, $\gamma \rightarrow -\gamma$. We can hence restrict ourselves to a given sign for γ . Without loss of generality, we choose $\gamma < 0$ and shall work with positive fields φ .

We plot in Fig. 8 the potential $v(\varphi)$ times κ as a function of $t = \sqrt{z_b} = \varphi\sqrt{\frac{8}{\kappa}}$ for several values of $h < 0$. For growing $|h|$ the potential becomes more asymmetric and its absolute minimum at $\sqrt{z_+} = \sqrt{\frac{8}{\kappa}}\varphi_+ = \Delta + |h|$ moves to the right.

As for the binomial inflaton potential with $m^2 < 0$ we can have here new or chaotic inflation depending on whether the initial field φ is in the interval $(0, \varphi_+)$ or in the interval $(\varphi_+, +\infty)$, respectively. In both cases the

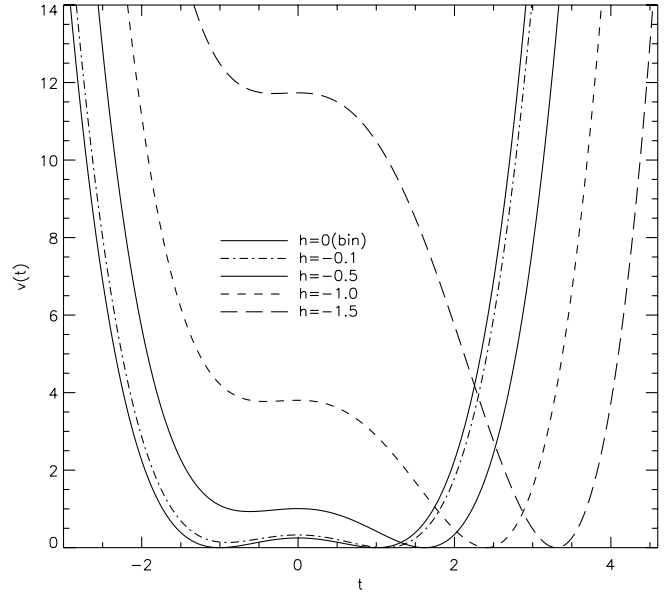


FIG. 8. The inflaton trinomial potential $\kappa v(\varphi)$ Eq. (3.23) vs. $t = \sqrt{z} = \varphi\sqrt{\frac{8}{\kappa}}$ for several values of $h < 0$. The absolute minimum moves to the right for growing $|h|$ and the potential becomes more and more asymmetric. $h \equiv \gamma\sqrt{\frac{8}{\kappa}} = \frac{g}{2\sqrt{\lambda}}$.

number of e-folds follows from Eqs. (3.3) and (3.23) where the field by the end of inflation is $\varphi_0 \simeq \varphi_+$. We thus find for the number of e-folds between the time τ and the end of inflation,

$$\kappa N(z_b) = z_b - 2h^2 - 1 - 2|h|\Delta + \frac{4}{3}|h|(|h| + \Delta - \sqrt{z_b})$$

$$+ \frac{16}{3}|h|(\Delta + |h|)\Delta^2 \log \left[\frac{1}{2} \left(1 + \frac{\sqrt{z_b} - |h|}{\Delta} \right) \right]$$

$$- 2w(h) \log[\sqrt{z_b}(\Delta - |h|)], \quad (3.26)$$

where $z_b = \frac{\kappa}{8}\varphi^2$ is defined by Eq. (3.9) and $w(h)$ is given by Eq. (3.25). In the variable z we have new inflation for $0 < z < z_+$ and chaotic inflation for $z_+ < z < +\infty$.

$\kappa N(z_b)$ in Eq. (3.26) as a function of z_b has its minimum at $z_b = z_+ \equiv \frac{\kappa}{8}\varphi_+^2 = 2h^2 + 1 + 2|h|\Delta$. This corresponds to $\sqrt{z_+} = \Delta + |h|$. When $\sqrt{z_b} \rightarrow \sqrt{z_+}$, $\kappa N(z_b)$ vanishes quadratically,

$$\kappa N(z_b) \stackrel{z_b \rightarrow z_+}{\simeq} 2(\sqrt{z_b} - \sqrt{z_+})^2 + \mathcal{O}[(\sqrt{z_b} - \sqrt{z_+})^3].$$

In the symmetric potential limit $h \rightarrow 0$, Eq. (3.26) reduces to Eq. (3.10) as it must be.

We obtain in analogous way from Eqs. (3.5) and (3.6) the spectral indices, r and the amplitude of adiabatic perturbations,

$$n_s = 1 - 6\kappa \frac{z_b(z_b + 2h\sqrt{z_b} - 1)^2}{[w(h) - 2z_b + \frac{8}{3}hz_b^{3/2} + z_b^2]^2} + \kappa \frac{3z_b + 4h\sqrt{z_b} - 1}{w(h) - 2z_b + \frac{8}{3}hz_b^{3/2} + z_b^2}, \quad (3.27)$$

$$r = 16\kappa \frac{z_b(z_b + 2h\sqrt{z_b} - 1)^2}{[w(h) - 2z_b + \frac{8}{3}hz_b^{3/2} + z_b^2]^2}, \quad (3.28)$$

$$|\delta_{kad}^{(S)}|^2 = \frac{1}{12\pi^2} \frac{|m^2|}{M_{\text{Pl}}^2 \kappa^2} \frac{[w(h) - 2z_b + \frac{8}{3}hz_b^{3/2} + z_b^2]^3}{z_b(z_b + 2h\sqrt{z_b} - 1)^2}. \quad (3.29)$$

The variable z_b is a function of κ times the number of e-folds N as defined by Eq. (3.26). Hence, Eqs. (3.27), (3.28), and (3.29) provide the spectral indices as functions of κN . In the $h \rightarrow 0$ limit these equations reduce to Eqs. (3.12) and (3.14) for the binomial potential as it must be.

The upper and lower bounds on the inflaton mass ratio $x = 10^6(m/M_{\text{Pl}})$ derived from Eq. (3.29) take the same form as Eq. (3.17)

$$\frac{200\sqrt{3}\pi}{N} g_b(z_b)\sqrt{\Delta_-} < x < \frac{200\sqrt{3}\pi}{N} g_b(z_b)\sqrt{\Delta_+}, \quad (3.30)$$

with the function,

$$g_b(z_b) = \frac{\kappa N \sqrt{z_b} |1 - 2h\sqrt{z_b} - z_b|}{[w(h) - 2z_b + \frac{8}{3}hz_b^{3/2} + z_b^2]^{3/2}}. \quad (3.31)$$

Figures 9, 12, and 15, depict, respectively, the central value for x Eq. (3.30), n_s Eqs. (3.26) and (3.27) and r Eqs. (3.26) and (3.28) as functions of $y = \kappa N$ for different values of $h < 0$ for the trinomial potential Eq. (3.23). In all cases the spectrum turns to be red tilted ($n_s < 1$).

The three-dimensional plots (10, 13, and 16) and (11, 14, and 17), display x , n_s and r as functions of $y = \kappa N$ and $h < 0$, for chaotic and new inflation, respectively.

Figure 18 depicts r as a function of n_s for new inflation with the trinomial potential Eq. (3.23) for different values of $h < 0$ as given by Eqs. (3.26) and (3.28). We see that r decreases when n_s goes below unit, as in the binomial case. In addition, r decreases for increasing asymmetry $|h|$ at a fixed n_s (with $h < 0$). Therefore, the trinomial potential Eq. (3.23) can yield very small r with $n_s < 1$ and near unit for new inflation [see Eq. (3.34)]. In this case we have the upper bound $r \leq \frac{8}{N} \approx 0.16$ [see Fig. 15 and Eq. (3.32)].

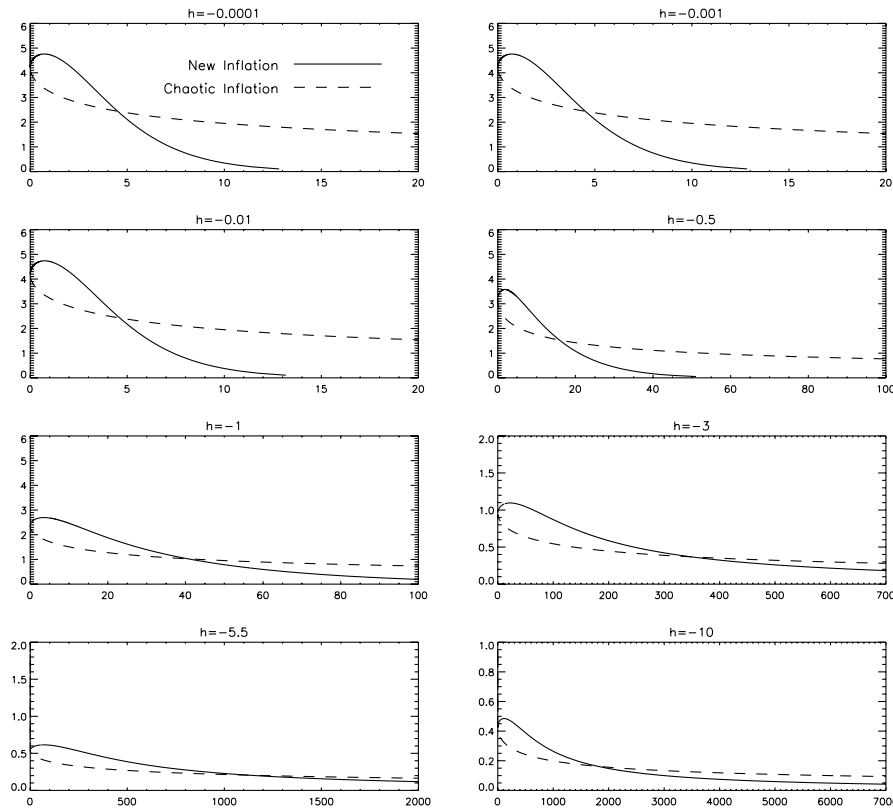


FIG. 9. The central value for $x = 10^6(m/M_{\text{Pl}})$ as a function of $y = \kappa N$ for different values of $h < 0$ and $N = 60$ with the trinomial potential Eq. (3.23) as given by Eq. (3.30). The upper branches correspond to new inflation while the lower branches correspond to chaotic inflation (compare with Fig. 12). Notice that the upper and lower bounds for x differ from the central value in only $\pm 6\%$.

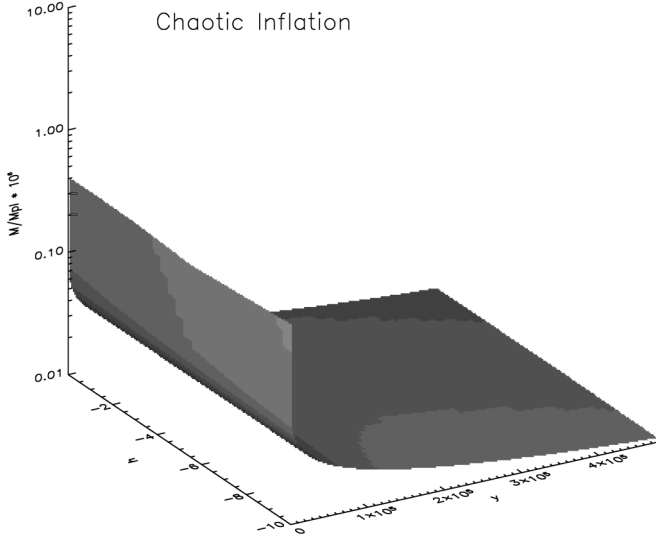


FIG. 10. The central value for $x = 10^6(m/M_{\text{Pl}})$ as a function of $y = \kappa N$ for $h < 0$ and $N = 60$ with the trinomial potential Eq. (3.23) as given by Eq. (3.30) for chaotic inflation. Notice that the upper and lower bounds for x differ from the central value in only $\pm 6\%$.

The three-dimensional plot of Fig. 19 depicts n_s as a function of r and h with the trinomial potential Eq. (3.23) as given by Eqs. (3.26), (3.27), and (3.28) for new inflation.

In Figs. 20 and 21 we plot r as function of n_s and h for chaotic inflation for the trinomial potential Eq. (3.23). We see that r increases when n_s goes below unit, as in the binomial case. For chaotic inflation with the trinomial potential Eq. (3.23) we have the lower bound $r \geq \frac{8}{N}$ [see Fig. 15 and Eq. (3.32)]. Notice that Fig. 20 displays a very small range of variation for n_s and r , actually, r as a

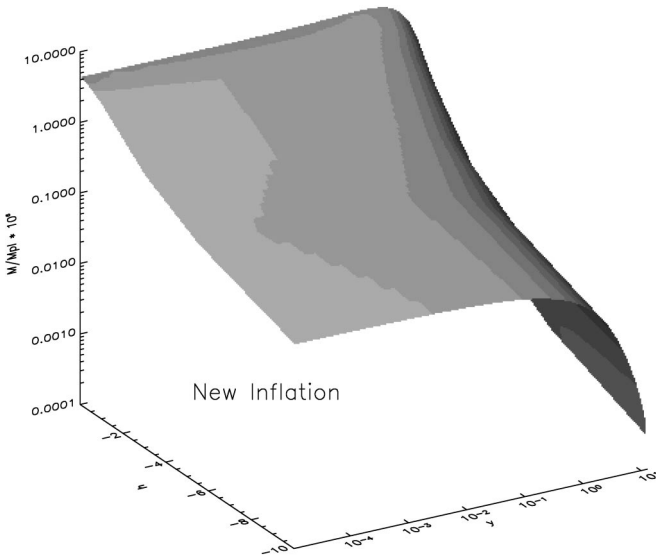


FIG. 11. The central value for $x = 10^6(m/M_{\text{Pl}})$ as a function of $y = \kappa N$ for $N = 60$ and $h < 0$ with the trinomial potential Eq. (3.23) as given by Eq. (3.30) for new inflation.

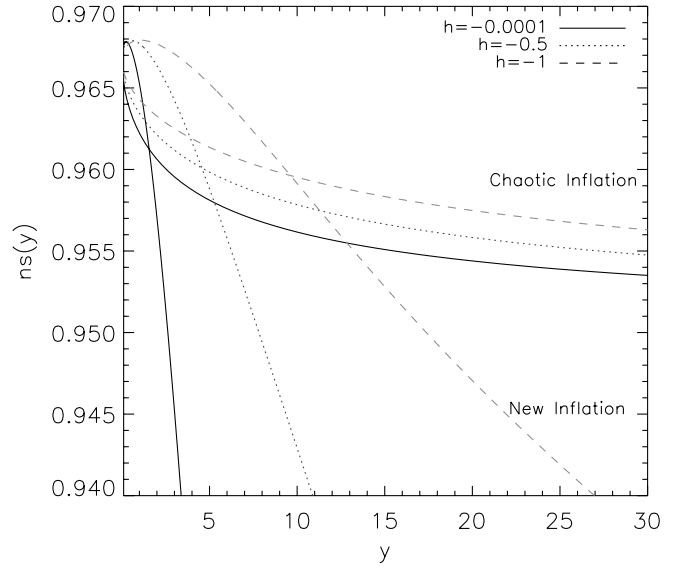


FIG. 12. n_s as a function of $y = \kappa N$ for $N = 60$ and different values of $h < 0$ with the trinomial potential Eq. (3.23) as given by Eqs. (3.26) and (3.27). The upper branches correspond to new inflation while the lower branches correspond to chaotic inflation.

function of n_s has a very weak dependence on the asymmetry $h < 0$ for chaotic inflation.

1. Limiting cases

Let us now consider the limiting cases: the shallow limit ($\kappa \rightarrow 0$) and the steep limit $\kappa \rightarrow \infty$.

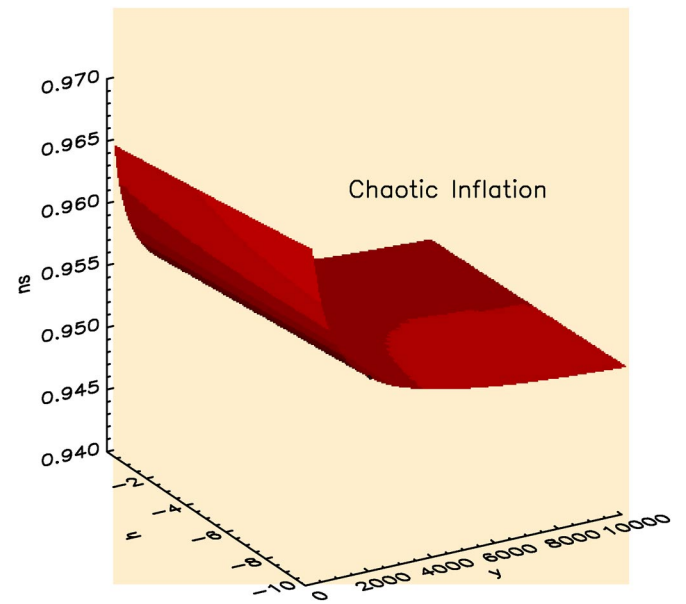


FIG. 13 (color online). n_s as a function of $y = \kappa N$ for $N = 60$ and $h < 0$ with the trinomial potential Eq. (3.23) as given by Eqs. (3.26) and (3.27) for chaotic inflation.

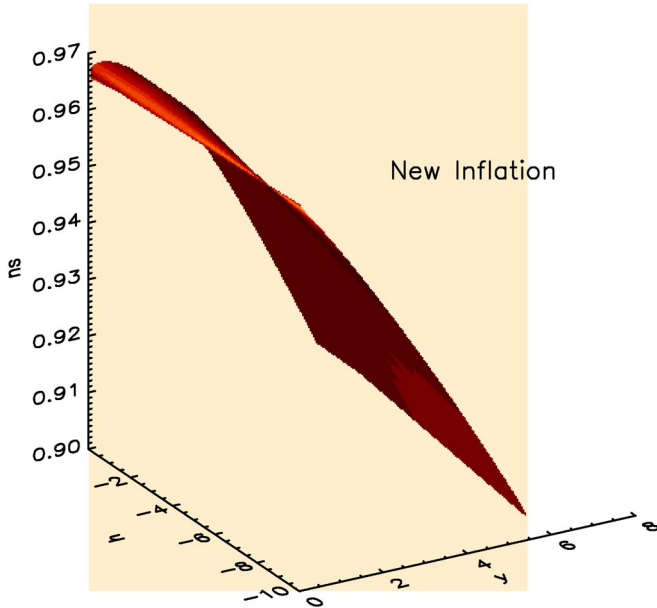


FIG. 14 (color online). n_s as a function of $y = \kappa N$ for $N = 60$ and $h < 0$ with the trinomial potential Eq. (3.23) as given by Eqs. (3.26) and (3.27) for new inflation.

In the shallow limit $\kappa \rightarrow 0$, $\kappa N(z_b)$ tends to its minimum $z_b = z_+$. We find from Eqs. (3.27) and (3.28)

$$n_s \stackrel{\kappa \rightarrow 0}{\approx} 1 - \frac{2}{N} \approx 0.96, \quad r \stackrel{\kappa \rightarrow 0}{\approx} \frac{8}{N} \approx 0.16 \quad (3.32)$$

which coincide with n_s and r Eq. (3.20) for the monomial

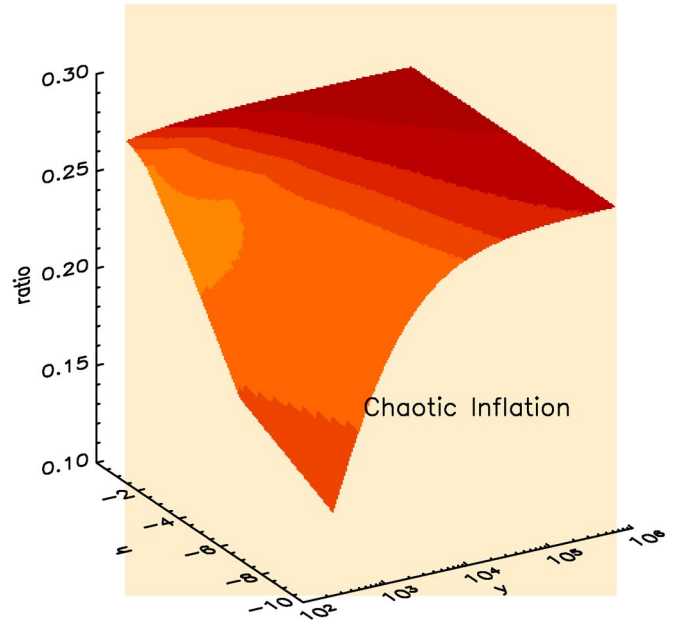


FIG. 16 (color online). r as a function of $y = \kappa N$ for $N = 60$ and $h < 0$ with the trinomial potential Eq. (3.23) as given by Eqs. (3.26) and (3.28) for chaotic inflation.

quadratic potential. That is, the $\kappa \rightarrow 0$ limit is h -independent as expected since for fixed h , $\gamma \stackrel{\kappa \rightarrow 0}{\approx} \mathcal{O}(\sqrt{\kappa})$ and the inflaton potential Eq. (3.23) becomes purely quadratic.

In the steep limit $\kappa \rightarrow \infty$ we have two possibilities: for new inflation z_b tends to zero while for chaotic inflation z_b tends to infinity.

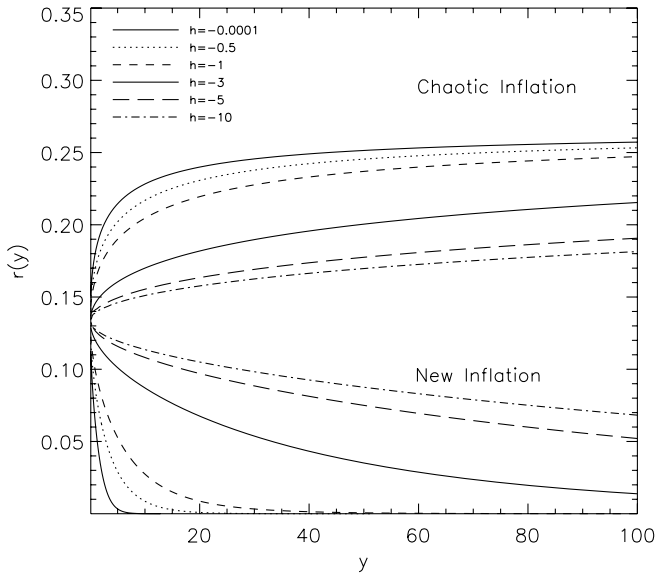


FIG. 15. r as a function of $y = \kappa N$ for $N = 60$ and different values of $h < 0$ with the trinomial potential Eq. (3.23) as given by Eqs. (3.26), (3.27), and (3.28). The upper branches correspond to chaotic inflation while the lower branches correspond to new inflation. Notice that $r > \frac{8}{N} \approx 0.16$ for chaotic inflation while $r < \frac{8}{N}$ for new inflation.

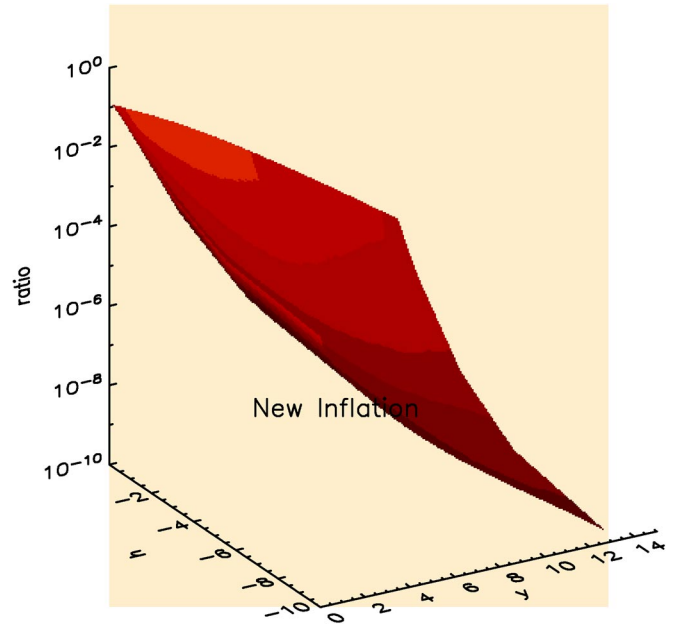


FIG. 17 (color online). r as a function of $y = \kappa N$ for $N = 60$ and $h < 0$ with the trinomial potential Eq. (3.23) as given by Eqs. (3.26) and (3.28) for new inflation.

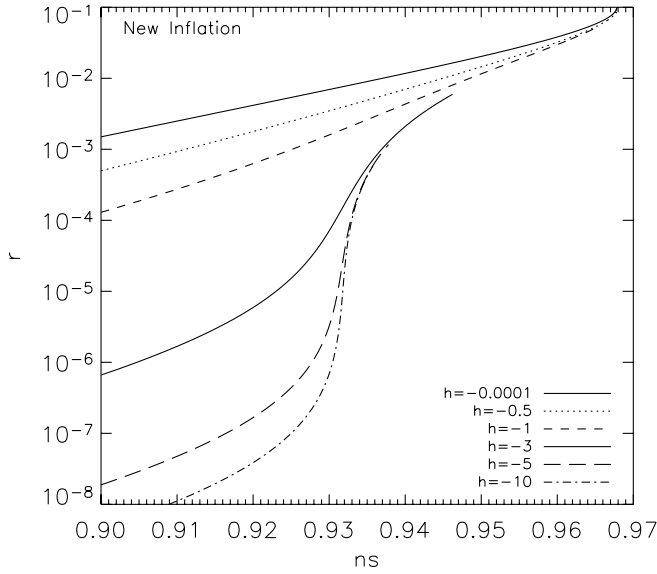


FIG. 18. r as a function of n_s for different values of $h < 0$ with the trinomial potential Eq. (3.23) as given by Eqs. (3.26), (3.27), and (3.28) for new inflation.

For new inflation we find from Eq. (3.26)

$$\kappa N(z_b) \stackrel{z_b \rightarrow 0}{=} -w(h) \log z_b - q(h) - 1 + \mathcal{O}(\sqrt{z_b}) \quad (3.33)$$

new inflation,

where

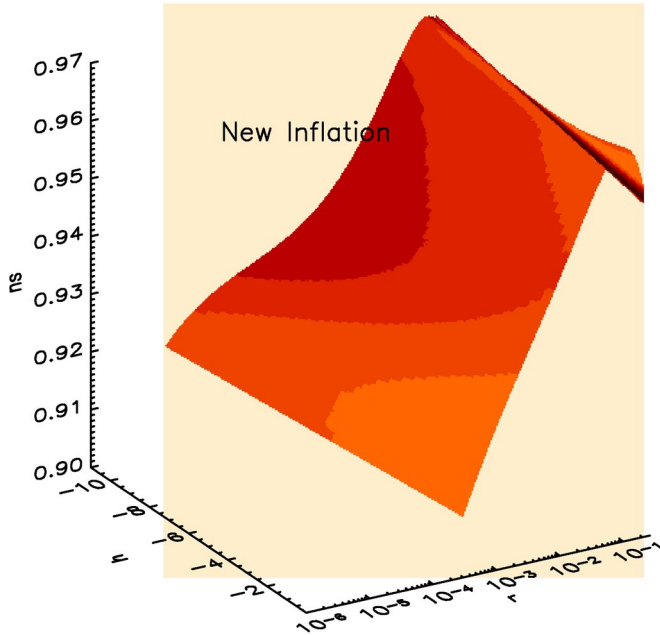


FIG. 19 (color online). n_s as a function of r and $h < 0$ with the trinomial potential Eq. (3.23) as given by Eq. (3.26) and (3.28) for new inflation.

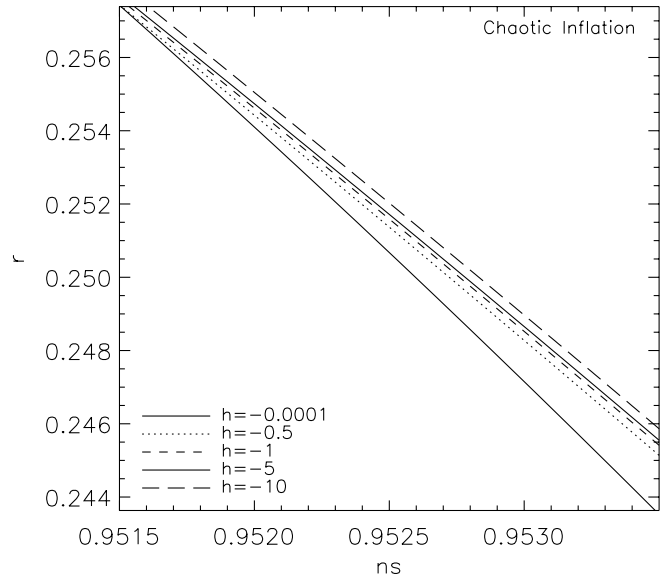


FIG. 20. r as a function of n_s for different values of $h < 0$ with the trinomial potential Eq. (3.23) as given by Eq. (3.26) and (3.28) for chaotic inflation.

$$q(h) \equiv 2w(h) \log[\Delta - |h|] - \frac{2}{3}(h^2 + |h|\Delta) \times \left\{ 8\Delta^2 \log\left[\frac{1}{2}\left(1 - \frac{|h|}{\Delta}\right)\right] - 1 \right\},$$

is a monotonically increasing function of the asymmetry $|h|$: $0 \leq q(h) < \infty$ for $0 < |h| < \infty$.

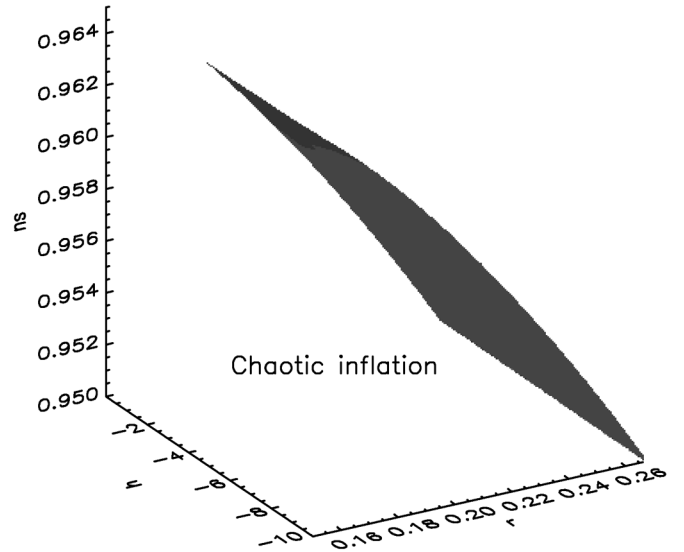


FIG. 21 (color online). n_s as a function of r and $h < 0$ with the trinomial potential Eq. (3.23) as given by Eq. (3.27) and (3.28) for chaotic inflation.

Then, Eqs. (3.27) and (3.28) yield,

$$n_s \stackrel{\kappa \gg 1}{\cong} 1 - \frac{\kappa}{w(h)},$$

$$r \stackrel{\kappa \gg 1}{\cong} 16 \frac{\kappa}{w^2(h)} e^{-[\kappa N + 1 + q(h)]/w(h)} \quad \text{new inflation} \quad (3.34)$$

In the $h \rightarrow 0$ limit we recover from Eqs. (3.33) and (3.34) the results for new inflation with a purely quartic potential Eq. (3.22) since $w(0) = 1$ and $q(0) = 0$.

We find for the function $g_b(z_b)$ governing the inflaton mass ratio Eq. (3.31)

$$g_b(z_b) \stackrel{\kappa \gg 1}{\cong} \frac{\kappa N}{w^{3/2}(h)} e^{-[\kappa N + 1 + q(h)]/2w(h)}, \quad \text{new inflation} \quad (3.35)$$

or using Eq. (3.34),

$$g_b(z_b) \stackrel{\kappa \gg 1}{\cong} \frac{N}{4} \sqrt{r(1 - n_s)}. \quad (3.36)$$

This implies for the mass ratio bounds in Eq. (3.30)

$$50\sqrt{3}\pi\sqrt{r(1 - n_s)}\sqrt{\Delta_-} < x < 50\sqrt{3}\pi\sqrt{r(1 - n_s)}\sqrt{\Delta_+}.$$

or

$$x = 127\sqrt{r(1 - n_s)} \pm 6\%. \quad (3.37)$$

We find in this limiting case that the mass ratio is directly related to the observable quantities n_s and r . For example, if $1 - n_s \sim r \sim 10^{-n}$, then $x \sim 10^{2-n}$.

Notice that in all cases the values of $n_s - 1$ and r are of the order $\frac{1}{N}$.

We read from Figs. 12 and 15 the behavior of n_s and r in chaotic and new inflation ($h < 0$):

- (i) Both for chaotic and new inflation n_s decreases with the steepness κ for fixed asymmetry $h < 0$ and grows with the asymmetry $|h|$ for fixed steepness κ .
- (ii) For chaotic inflation r grows with the steepness κ for fixed asymmetry $h < 0$ and decreases with the asymmetry $|h|$ for fixed steepness κ . For new inflation r does the opposite: it decreases with the steepness κ for fixed asymmetry $h < 0$ while it grows with the asymmetry $|h|$ for fixed steepness κ .

From Figs. 9, 12, and 15 we can understand how the mass ratio m/M_{Pl} varies with n_s and r . For chaotic inflation we have $r \geq \frac{8}{N}$ and $10^5(m/M_{\text{Pl}})$ stays larger than unit in order to keep n_s in the observed WMAP range. For new inflation, we have $r \leq \frac{8}{N}$ and m/M_{Pl} decreases for decreasing r . However, if we consider $10^5(m/M_{\text{Pl}}) < 1$ say, Eq. (3.37) and Figs. 9, 12, and 15 show that $(1 - n_s)r$ must be $\sim 10^{-6}$ which is probably a too small value. That is, there is a limiting value for the inflaton mass $x_0 \equiv 10^6 m_0/M_{\text{Pl}} \approx 0.1$ such that $m_0 \approx 10^{-7} M_{\text{Pl}}$ is a minimal inflaton mass in order to keep n_s and r within the WMAP data.

This concludes our discussion of the trinomial inflaton potential with $m^2 < 0$. The case $m^2 > 0$ can be treated analogously and yields results conceptually similar to the binomial potential: one finds chaotic inflation modulated by the asymmetry parameter h . We shall not consider such case here since it yields, as always in chaotic inflation, a ratio $r > \frac{8}{N}$.

IV. HYBRID INFLATION

In the inflationary models of hybrid type, the inflaton is coupled to another scalar field σ_0 through a potential of the type [19]

$$V_{\text{hyb}}(\phi, \sigma_0) = \frac{m^2}{2} \phi^2 + \frac{g_0^2}{2} \phi^2 \sigma_0^2 + \frac{\mu_0^4}{16\Lambda_0} \left(\sigma_0^2 - \frac{4\Lambda_0}{\mu_0^2} \right)^2$$

$$= \frac{m^2}{2} \phi^2 + \Lambda_0 + \frac{1}{2} (g_0^2 \phi^2 - \mu_0^2) \sigma_0^2$$

$$+ \frac{\mu_0^4}{16\Lambda_0} \sigma_0^4. \quad (4.1)$$

where $\mu_0^2 > 0$ is of the order $m^2 > 0$, $\Lambda_0 > 0$ plays the role of a cosmological constant and g_0^2 couples σ_0 with ϕ .

The initial conditions are chosen such that σ_0 and $\dot{\sigma}_0$ are very small and one can therefore consider,

$$V_{\text{hyb}}(\phi, 0) = \frac{m^2}{2} \phi^2 + \Lambda_0. \quad (4.2)$$

One has then inflation driven by the cosmological constant Λ_0 in the regime $\phi(0) \ll \sqrt{\Lambda_0}$. The inflaton field $\phi(t)$ decreases with time while the scale factor $a(t)$ grows exponentially. We see from Eq. (4.1) that

$$m_\sigma^2 = g_0^2 \phi^2 - \mu_0^2$$

plays the role of a effective classical mass square for the field σ_0 . The initial value of m_σ^2 depends on the initial conditions but is typically positive. Anyway, since in chaotic inflation the inflaton field ϕ decreases with time, m_σ^2 will be necessarily negative at some moment during inflation. At such moment, spinodal (tachyonic) unstabilities appear and the field σ starts to grow exponentially until it dominates the energy of the universe. Inflation stops at such time and then after, a matter dominated regime follows.

Hybrid inflation can also be obtained with other couplings like

$$\tilde{V}_{\text{hyb}}(\phi, \sigma_0) = \frac{m^2}{2} \phi^2 + \Lambda_0 + \frac{1}{2} (2mg_0\phi - \mu_0^2) \sigma_0^2 + \frac{\tilde{g}}{4} \sigma_0^4. \quad (4.3)$$

where g_0 couples σ_0 with ϕ , and the quartic coupling $\tilde{g} > 2g_0^2$ ensures the stability of the model. Here, the effective classical mass square for σ_0 reads,

$$m_\sigma^2 = 2mg_0\phi - \mu_0^2.$$

Again m_σ^2 becomes negative at some moment of inflation due to the fact that the inflaton field ϕ decreases with time. Spinodal instabilities are then triggered and inflation eventually stops followed by a matter dominated regime. As for the potential $V_{\text{hyb}}(\phi, \sigma_0)$, in the regime $\phi(0) \ll \sqrt{\Lambda_0}$, inflation is driven by the cosmological constant Λ_0 [20].

In hybrid inflation the role of the field σ_0 is to stop inflation. This field is negligible when the relevant cosmological scales cross out the horizon. Hence, σ_0 does not affect the spectrum of density and tensor fluctuations except through the number of e-folds.

The evolution equations in dimensionless variables for the model $V_{\text{hyb}}(\phi, \sigma_0)$ Eq. (4.1) take the form

$$\begin{aligned} h^2(\tau) &= \frac{2}{3} \left[\dot{\phi}^2 + \varphi^2 + \frac{\mu^4}{4\Lambda} \left(\sigma^2 - \frac{2\Lambda}{\mu^2} \right)^2 + g^2 \sigma^2 \varphi^2 \right], \\ \dot{\phi} + 3h\dot{\phi} + \varphi + g^2 \sigma^2 \varphi &= 0, \\ \ddot{\sigma} + 3h\dot{\sigma} - \mu^2 \sigma + g^2 \sigma \varphi^2 + \frac{r^2}{2\Lambda} \sigma^3 &= 0. \end{aligned} \quad (4.4)$$

where

$$\begin{aligned} \sigma(\tau) &\equiv \frac{\sigma_0(t)}{M_{\text{Pl}}}, & g^2 &\equiv g_0^2 \frac{M_{\text{Pl}}^2}{m^2}, & \mu^2 &\equiv \frac{\mu_0^2}{m^2} \\ \text{and } \Lambda &\equiv \frac{2\Lambda_0}{m^2 M_{\text{Pl}}^2}. \end{aligned}$$

In the slow-roll and Λ -dominated regime:

$$\dot{\phi}(0) \ll m\phi(0) \ll \sqrt{\Lambda},$$

we can neglect the field σ and approximate the evolution Eqs. (4.4) by

$$3h\dot{\phi} + \varphi = 0, \quad h^2(\tau) = \frac{2}{3} [\varphi^2 + \Lambda]. \quad (4.5)$$

The number of e-folds from the time τ until the end of inflation is then given by Eq. (3.3),

$$\begin{aligned} N(\tau) &= \int_0^\tau h(\tau) d\tau = - \int_{\varphi(\tau)}^{\varphi_0} \frac{v(\varphi)}{v'(\varphi)} d\varphi \\ &= \frac{1}{4} [\varphi^2(\tau) - \varphi_0^2] + 2\Lambda \log \frac{\varphi(\tau)}{\varphi_0} \end{aligned} \quad (4.6)$$

where φ_0 is the inflaton field by the end of inflation. We have verified this approximation by integrating numerically Eqs. (4.4).

We see that the field and its dynamics only appears in Eq. (4.6) through the value of φ_0 where inflation stops. The value of φ_0 follows by solving Eqs. (4.4) and depends on the initial conditions as well as on the parameters g, μ and Λ .

For $\Lambda \rightarrow 0$ hybrid inflation becomes chaotic inflation with the monomial potential $\frac{1}{2}\varphi^2$. In that limit Eq. (4.6) becomes Eq. (3.7) with $\kappa \rightarrow 0$ as it should be.

The spectral indices are given by Eqs. (3.4) and (3.5) and the amplitude of adiabatic perturbations by Eq. (3.6). By using the potential Eq. (4.2) in dimensionless variables we find,

$$\begin{aligned} v(\varphi, 0) &= \frac{1}{2}(\varphi^2 + \Lambda), & \eta &= \frac{2}{\varphi^2 + \Lambda}, \\ \epsilon &= \frac{2\varphi^2}{(\varphi^2 + \Lambda)^2}, \end{aligned} \quad (4.7)$$

$$|\delta_{kad}^{(S)}|^2 = \frac{1}{96\pi^2} \left(\frac{m}{M_{\text{Pl}}} \right)^2 \frac{(\varphi^2 + \Lambda)^3}{\varphi^2}, \quad (4.8)$$

$$n_s = 1 + 4 \frac{\Lambda - 2\varphi^2}{(\varphi^2 + \Lambda)^2}, \quad r = 32 \frac{\varphi^2}{(\varphi^2 + \Lambda)^2}.$$

where φ is the inflaton at the moment of the first horizon crossing.

Since $\varphi \ll \sqrt{\Lambda}$ Eq. (4.7) and (4.8) simplify as,

$$\begin{aligned} \eta &= \frac{2}{\Lambda}, & \epsilon &= 2 \left(\frac{\varphi}{\Lambda} \right)^2, \\ |\delta_{kad}^{(S)}|^2 &= \frac{1}{96\pi^2} \left(\frac{m}{M_{\text{Pl}}} \right)^2 \left(\frac{\Lambda}{\varphi} \right)^2 \Lambda, \end{aligned} \quad (4.9)$$

$$n_s = 1 + \frac{4}{\Lambda} - 12 \frac{\varphi^2}{\Lambda^2}, \quad r = 32 \frac{\varphi^2}{\Lambda^2}.$$

In terms of the variable $x = 10^6(m/M_{\text{Pl}})$ [Eq. (3.16)] we get

$$\begin{aligned} \frac{\varphi^2}{\Lambda^2} &= \frac{1}{96\pi^2} \frac{x^2}{|\delta_{kad}^{(S)}|^2} 10^{-12} \Lambda = 0.478 \times 10^{-6} x^2 \Lambda, \\ \frac{r}{\Lambda} &= \frac{1}{3\pi^2} \frac{x^2}{|\delta_{kad}^{(S)}|^2} 10^{-12} = 1.5210^{-5} x^2, \end{aligned} \quad (4.10)$$

where we used the WMAP data for the amplitude of scalar perturbations Eq. (3.19). Since,

$$n_s = 1 + \frac{4}{\Lambda} - \frac{3}{8} r, \quad (4.11)$$

we find from Eqs. (4.10) and (4.11),

$$\begin{aligned} x &= 10^6 \frac{m}{M_{\text{Pl}}} = 5\pi\sqrt{3}10^5 |\delta_{kad}^{(S)}| \sqrt{r(1 - n_s)} \\ &= 127 \sqrt{r(n_s - 1 + \frac{3}{8}r)}, \end{aligned} \quad (4.12)$$

$$\frac{\Lambda_0^{1/4}}{M_{\text{Pl}}} = 0.0135 r^{1/4},$$

$$\frac{\Lambda_0}{M_{\text{Pl}}^4} = 0.329 \times 10^{-7} r.$$

Notice that the expression for the mass ratio has a similar structure than for new inflation (in the limiting case) Eq. (3.37). In Figs. 22 and 23 we plot $x = 10^6(m/M_{\text{Pl}})$ as a function of n_s and r according to Eq. (4.12). We see that

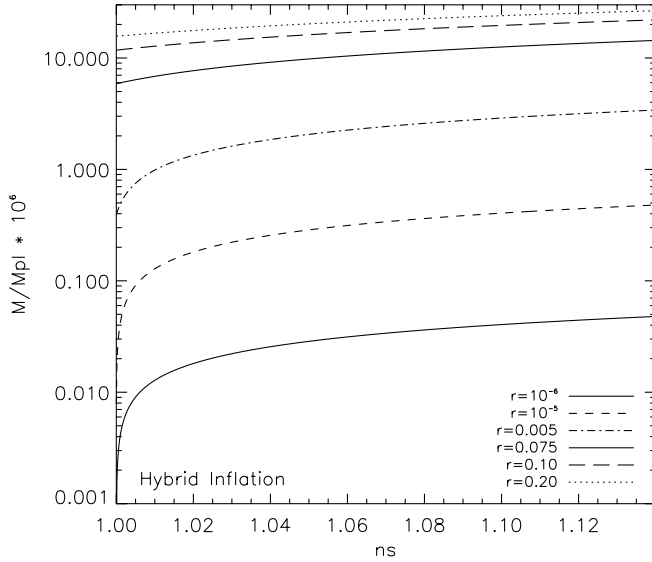


FIG. 22. $x = 10^6(m/M_{\text{Pl}})$ as a function of n_s for different values of r in hybrid inflation according to Eq. (4.12).

m/M_{Pl} decreases when r and $n_s - 1$ both approach zero. Figure 24 displays n_s and r as functions of Λ for a fixed x according to Eqs. (4.10) and (4.11).

From Eq. (4.8) we obtain φ^2 as a function of n_s and Λ ,

$$\varphi_{\pm}^2 = -\Lambda + \frac{4}{n_s - 1} \left[-1 \pm \sqrt{1 + \frac{3}{4} \Lambda (n_s - 1)} \right]. \quad (4.13)$$

We see that φ_+^2 is positive and hence physical for $n_s > 1$ and $\Lambda < 4/(n_s - 1)$ while φ_-^2 is positive and hence physical for $n_s < 1$ and $\Lambda < 4/(3|n_s - 1|)$. Hence, the value of $n_s - 1$ gives an upper bound on the cosmological constant

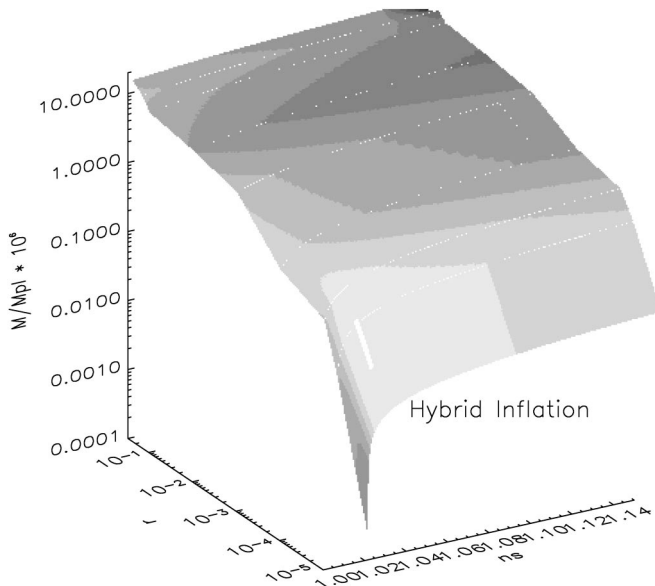


FIG. 23. $x = 10^6(m/M_{\text{Pl}})$ as a function of n_s and r in hybrid inflation according to Eq. (4.12)

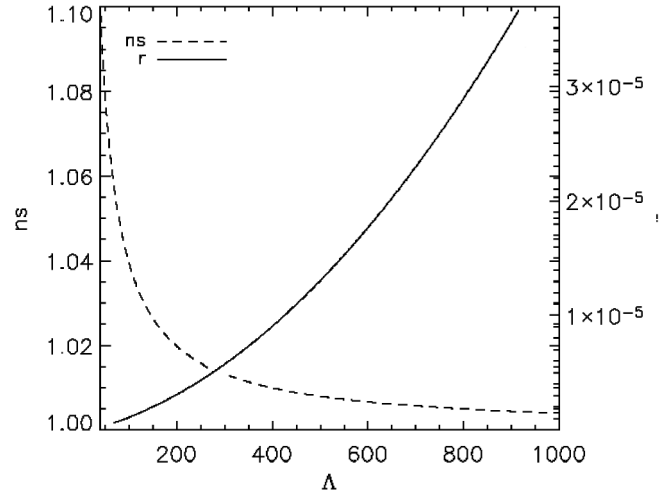


FIG. 24. n_s and r as functions of Λ for a fixed x according to Eqs. (4.10) and (4.11). Here, $x = 0.0411$.

Λ . In addition, one sees from Eq. (4.8) that we have for hybrid inflation

$$n_s - 1 - \frac{4}{\Lambda} < 0 \quad \text{for all } \varphi^2 > 0.$$

Moreover, when $\Lambda \gg \varphi^2$ (Λ -dominated regime), we see from Eq. (4.8) that the spectrum exhibits a blue tilt ($n_s > 1$). [Both chaotic and new inflation yield red tilted spectra ($n_s < 1$) as discussed in sec. III].

We see from Eqs. (4.6) and (4.9) that $\Lambda \sim N$ and hence

$$n_s - 1 = \mathcal{O}\left(\frac{1}{N}\right), \quad r = \mathcal{O}\left(\frac{1}{N^2}\right).$$

V. CONCLUSIONS AND IMPLICATIONS FOR SUPERSYMMETRY AND STRING THEORY

Setting the inflaton mass $m = 0$ in polynomial potentials like Eq. (2.5) implies a highly particular nongeneric choice. WMAP [7] unfavors such a choice and supports a generic polynomial potential. Actually, we find that the fact that the pure ϕ^4 potential is disfavored implies a lower bound on m . As discussed in secs. III and IV one gets $m \gtrsim 10^{13}$ GeV.

The potential which best fits the present data for red tilted spectrum ($n_s < 1$) and which best prepares the way to the expected data (a small $r \lesssim 0.1$) is given by the trinomial potential Eq. (1.1) with a negative φ^2 term, that is new inflation. In new inflation we have the upper bound $r \leq \frac{8}{N} \approx 0.16$.

The data on the spectral indices should be able to make soon a clear selection between inflationary models: we see that a measured upper bound $r \lesssim 0.16$ excludes chaotic inflation. If this happens to be the case, then whether n_s turns to be above or below unit will exclude either new or hybrid inflation, respectively.

The grand unification idea consists in that at some energy scale all three couplings (electromagnetic, weak and strong) should become of the same strength. In this case, such grand unified scale turns out to be $E \sim 10^{16}$ GeV [21,22]. The running of the couplings with the energy (or the length) is governed by the renormalization group. For the standard model of electromagnetic, weak and strong interactions, the renormalization group yields that the three couplings get unified approximately at $\sim 10^{16}$ GeV. A better convergence is obtained in supersymmetric extensions of the standard model [21,22].

Neutrino oscillations and neutrino masses are currently explained in the seesaw mechanism as follows [23],

$$\Delta m_\nu \sim \frac{M_{\text{Fermi}}^2}{M}$$

where $M_{\text{Fermi}} \sim 250$ GeV is the Fermi mass scale, $M \gg M_{\text{Fermi}}$ is a large energy scale and Δm_ν is the difference between the neutrino masses for different flavors. The observed values for $\Delta m_\nu \sim 0.009 - 0.05$ eV naturally call for a mass scale $M \sim 10^{15-16}$ GeV close to the GUT scale [23].

Equation (2.8) for the inflaton potential resembles the moduli potential coming from supersymmetry breaking,

$$V_{\text{susy}}(\phi) = m_{\text{susy}}^4 v \left(\frac{\phi}{M_{\text{Pl}}} \right), \quad (5.1)$$

where m_{susy} stands for the supersymmetry breaking scale. Potentials with such form were used in the inflationary context in refs.[24]. In our context, Eq. (5.1) implies that $m_{\text{susy}} \sim 10^{16}$ GeV. That is, the susy breaking scale m_{susy} turns out to be at the GUT scale $m_{\text{susy}} \sim M_{\text{GUT}}$.

We see that the mass scale of the inflaton $m \sim 10^{13}$ GeV can be related with M_{GUT} by a seesaw style relation,

$$m \sim \frac{M_{\text{GUT}}^2}{M_{\text{Pl}}}. \quad (5.2)$$

As discussed in secs. I and II the inflaton describes a condensate in a GUT theory in which it may describe fermion-antifermion pairs. Current identifications in the literature of such condensate field with a given fundamental field in a SUSY or SUGRA model have so far no solid basis. Moreover, the number of supersymmetric models is so large that there is practically no way to predict which is the correct model [25].

In order to generate inflation in string theory one needs first to generate a mass scale like the inflaton mass $m \sim 10^{13}$ GeV. Such scale is not present in the string action, neither in the action of the effective background fields (dilaton, graviton, antisymmetric tensor) which are massless. Without the presence of the mass scales m and M_{GUT} [related through Eq. (5.2)], there is no hope in string theory to get a correct inflationary cosmology describing the observed CMB fluctuations [14]. Such scale should be generated dynamically perhaps from the string vacuum (ua) but this is still an open problem far from being solved [14]. Actually, the very same problem hinders the derivation of a GUT theory and the generation of the GUT scale from string theory.

Since no microscopic derivation of an inflationary model from a GUT is available so far, it would seem too ambitious at this stage to look for a microscopic derivation of inflation from string theory. The derivation of an inflationary cosmology reproducing the observed CMB fluctuations is at present too far away in string theory. However, an effective description of inflation in string theory (string matter plus massless backgrounds) could be at reach [14].

-
- [1] A. Guth, Phys. Rev. D **23**, 347 (1981); astro-ph/0404546.
 - [2] E. W. Kolb and M. S. Turner, *The Early Universe* (Addison Wesley, Redwood City, CA, 1990).
 - [3] P. Coles and F. Lucchin, *Cosmology* John (Wiley, Chichester, 1995).
 - [4] A. R. Liddle and D. H. Lyth, *Cosmological Inflation and Large Scale Structure* (Cambridge University Press, Cambridge, England, 2000).
 - [5] D. H. Lyth and A. Riotto, Phys. Rep. **314**, 1 (1999).
 - [6] G. F. Smoot *et al.*, Astrophys. J. Lett. **396**, L1 (1992).
 - [7] C. L. Bennett *et al.* (WMAP Collaboration), Astrophys. J. Suppl. Ser. **148**, 1 (2003); A. Kogut *et al.* (WMAP Collaboration), Astrophys. J. Suppl. Ser. **148**, 161 (2003); D. N. Spergel *et al.* (WMAP Collaboration), Astrophys. J. Suppl. Ser. **148**, 175 (2003); H. V. Peiris *et al.* (WMAP Collaboration), Astrophys. J. Suppl. Ser. **148**, 213 (2003).
 - [8] M. S. Turner, Phys. Rev. D **48**, 3502 (1993); S. Dodelson, W. H. Kinney, and E. W. Kolb, Phys. Rev. D **56**, 3207 (1997); S. M. Leach, A. R. Liddle, J. Martin, and D. J. Schwarz, Phys. Rev. D **66**, 023515 (2002); N. Bartolo, S. Matarrese, and A. Riotto, Phys. Rev. D **64**, 083514 (2001); N. Bartolo, E. Komatsu, S. Matarrese, and A. Riotto, Phys. Rep. **402**, 103 (2004).
 - [9] See, for example, W. Hu and S. Dodelson, Annu. Rev. Astron. Astrophys. **40**, 171 (2002); J. Lidsey, A. Liddle, E. Kolb, E. Copeland, T. Barreiro, and M. Abney, Rev. Mod. Phys. **69**, 373 (1997); W. Hu, astro-ph/0402060.
 - [10] V. A. Belinsky, L. P. Grishchuk, Ya. B. Zeldovich, and I. M. Khalatnikov, Phys. Lett. B **155**, 232 (1985); JETP Lett. **62**, 195 (1985).
 - [11] D. Boyanovsky and H. J. de Vega, in the *Proceedings of the VIIIth. Chalonge School*, edited by N. G. Sanchez (Kluwer Publishers, Dordrecht, 2001) Series C,

- Vol. 562, p. 37; D. Boyanovsky, D. Cormier, H. J. de Vega, R. Holman, and S.P. Kumar, Phys. Rev. D **57**, 2166 (1998); D. Boyanovsky, H.J. de Vega, and R. Holman, Phys. Rev. D **49**, 2769 (1994); D. Boyanovsky, F.J. Cao, and H. J. de Vega, Nucl. Phys. **B632**, 121 (2002).
- [12] F.J. Cao, H. J. de Vega, and N. G. Sanchez, Phys. Rev. D **70**, 083528 (2004).
- [13] D. Boyanovsky and H.J. de Vega, Phys. Rev. D **70**, 063508 (2004); D. Boyanovsky, H.J. de Vega, and N. Sánchez, Phys. Rev. D **71**, 023509 (2005).
- [14] H.J. de Vega and N. Sánchez, Phys. Rev. D **50**, 7202 (1994); H. J. de Vega and N. Sánchez, *Lectures on String Theory in Curved Spacetimes*, NATO Advanced Study Institute, Ser. B, Vol. 476 (Kluwer Academic Publishers, Dordrecht, 1995), p. 11; M.P. Infante and N. Sánchez, Phys. Rev. D **61**, 083515 (2000).
- [15] M. S. Turner, Ann. Inst. Henri Poincaré **4**, s333 (2003).
- [16] H. Leutwyler, Ann. Phys. (N.Y.) **235**, 165 (1994); S. Weinberg, hep-ph/9412326; S. Weinberg, *The Quantum Theory of Fields* (Cambridge University Press, Cambridge, England, 2000), Vol. 2.
- [17] H. M. Hodges, G. R. Blumenthal, L. A. Kofman, and J. R. Primack, Nucl. Phys. **B335**, 197 (1990).
- [18] L. Verde, astro-ph/0306272; S. M. Leach and A.R. Liddle, Phys. Rev. D **68**, 123508 (2003); V. Barger, H.S. Lee, and D. Marfatia, Phys. Lett. B **565**, 33 (2003); W.H. Kinney, E. W. Kolb, A. Melchiorri, and A. Riotto, Phys. Rev. D **69**, 103516 (2004); R. Rebolo *et al.*, astro-ph/0402466.
- [19] A. Linde, Phys. Rev. D **49**, 748 (1994); J. García Bellido and A. Linde, Phys. Rev. D **57**, 6075 (1998).
- [20] E. J. Copeland, A. R. Liddle, D. H. Lyth, E. D. Stewart, and D. Wands, Phys. Rev. D **49**, 6410 (1994).
- [21] N. Polonsky, *Supersymmetry Structure and Phenomena*, Lecture Notes in Physics Vol. M68 (Springer-Verlag, Heidelberg, 2001), p. 1.P. Langacker and N. Polonsky, Phys. Rev. D **47**, 4028 (1993). K. S. Babu, J. C. Pati, and F. Wilczek, Nucl. Phys. **B566**, 33 (2000).
- [22] S. Weinberg, *The Quantum Theory of Fields* (Cambridge University Press, Cambridge, England, 2000), Vol. 3.
- [23] See for recent reviews, R. D. Peccei, Nucl. Phys. B Proc. Suppl. **137**, 277 (2004); G. Altarelli and F. Feruglio, New J. Phys. **6**, 106 (2004).
- [24] F. C. Adams, J. R. Bond, K. Freese, J. A. Frieman, and A. V. Olinto, Phys. Rev. D **47**, 426 (1993); G. Dvali, Q. Shafi, and R. Schaefer, Phys. Rev. Lett. **73**, 1886 (1994); V. N. Senaguz and Q. Shafi, J. Phys. G **30**, S431 (2004); V. N. Senaguz and Q. Shafi, Phys. Rev. D **71**, 043514 (2005); L. Randall, M. Soljatic, and A. H. Guth, Nucl. Phys. **B472**, 377 (1996); K. Kadota and E. D. Stewart, J. High Energy Phys. 07 (2003) 013; J. High Energy Phys. 12 (2003) 008.
- [25] P. Ramond, hep-ph/0411010.